

The Role of Disintegrin and Metalloproteinase 15 (ADAM15) in Myocardial Infarction

**by
Michael Chute**

A thesis submitted in partial fulfillment of the requirements for the degree of

Master of Science

Department of Physiology

University of Alberta

© Michael Chute, 2020

Abstract

Ischemic cardiomyopathy remains the primary cause of heart failure worldwide. A disintegrin and metalloproteinases (ADAMs) are a family of membrane-bound proteases with diverse functions. ADAM15 is expressed in the myocardium and is involved in mechanisms associated with ischemic heart disease pathology, however, its function in ischemic heart disease remains unexplored. We investigated if ADAM15 is involved in the remodeling of the left ventricle after a MI was induced.

The research presented in this thesis identified the role of ADAM15 in left ventricular remodeling following myocardial infarction. Adult male wildtype (WT) and ADAM15-deficient (*Adam15*^{-/-}) mice were subjected to myocardial infarction (MI) by permanent ligation of the left anterior descending (LAD) artery. LV structure and function were assessed by echocardiography. *Adam15*^{-/-} mice exhibited significantly compromised survival post-MI, mainly due to LV rupture. Cardiac contractility was reduced in *Adam15*^{-/-} compared to WT-MI mice. Hearts were assessed at 3-days or 1-week post-MI, the start and end of the time period for LV rupture incidents, respectively. Collagen fibers in the scar tissue were distorted and scarce in *Adam15*^{-/-}-MI hearts (second harmonic generation imaging), associated with reduced levels of lysyl oxidase-1 (LOX-1), a major collagen cross-linking enzyme, and expression of fibronectin, a key extracellular matrix (ECM) protein. *In vitro* adult cardiac fibroblasts from *Adam15*^{-/-} hearts showed impaired myofibroblast transformation under ischemic conditions

(hypoxia+nutrition deletion), suggesting attenuated fibroblast activation. *In vivo* and *in vitro* molecular analyses revealed that interaction of ADAM15 with p21-activated kinase (PAK1) is required for induction of LOX-1 and fibronectin which are critical in optimal scar formation post-MI.

In summary, the research described in this dissertation demonstrates that ADAM15 is required for optimal scar formation following myocardial infarction. ADAM15-deficiency suppresses fibroblast activation and induction of LOX-1 and fibronectin, thereby impairing wound healing post-MI, by preventing FB activation leading to deleterious remodelling and LV rupture.

Preface

All of the work presented henceforth was conducted in Dr. Zamaneh Kassiri's laboratory in 474 Heritage Medical Research Centre, University of Alberta, Edmonton, AB, Canada. Non-failing human hearts were procured through the Human Organ Procurement and Exchange program (HOPE) at the University of Alberta (credit: Dr. Gavin Oudit). Failing ischemic hearts were procured through the Human Explanted Heart Program (HELP) at the Mazankowski Alberta Heart Institute (Edmonton, AB; credit: Dr. Gavin Oudit). All experiments were performed in accordance with the institutional ethics committee. Informed consent was obtained from study subjects. This research project received research ethics approval from the University of Alberta Research Ethics Board, "TIMPs and Myocardial Infarction & Breeding Colony", AUP396.

The induction of myocardial infarctions via left anterior descending ligation was performed by Dr. Wang Wang and Dr. Faqi Wang. Mrs. Jessica Worton (*née* DesAulniers) performed all quantitative TaqMan real-time PCR experiments. Dr. Thomas Abraham from the Department of Neural and Behavioral Sciences at Penn State performed the second harmonic generation imaging.

Dedication

To my parents, for their unconditional love and support throughout this process.

Acknowledgements

I would like to thank the following people, without whom I would not have been able to complete this research:

My supervisor Dr. Zamaneh Kassiri, for her contributions of time, ideas, patience and funding to make this degree possible.

My committee members Dr. Gary Lopaschuk and Dr. Carlos Fernandez-Patron, for challenging me to think outside of the box.

Dr. Gavin Oudit, for providing both resources and personnel to aid in the completion of experiments.

The members of the Kassiri group and Oudit group, for enabling me to ask questions and explore ideas.

The Cardiovascular Research Centre for their technical assistance and support.

And finally, my friends, for putting up with me for all these years.

Table of Contents

Chapter 1. Introduction	1
1.1 Introduction.....	2
1.2 Anatomy of the heart.....	2
1.3 Cell types in the heart.....	4
1.4 Ischemic cardiomyopathy.....	6
1.4.1 Epidemiology.....	7
1.4.2 Risk factors.....	9
1.4.3 Pathogenesis.....	10
1.4.4 Treatment of MI.....	17
1.5 Disintegrin and metalloproteinases: ADAMs.....	19
1.5.1 Pro-domain.....	20
1.5.2 Metalloproteinase.....	20
1.5.3 Disintegrin Domain.....	21
1.5.4 Cysteine-rich region.....	21
1.5.5 EGF-like domain.....	22
1.5.6 Cytoplasmic tail.....	22
1.6 ADAM15.....	23
1.7 Rationale.....	23
1.8 Hypothesis.....	24
1.9 Objectives.....	24
Chapter 2. Materials and Methods.....	25
2.1 Animals and surgical procedure.....	26

2.2 Human explanted heart tissue.....	26
2.3 Echocardiography and strain assessments.....	27
2.4 Histochemical and immunostaining analysis.....	28
2.5 Protein and mRNA extraction and analysis.....	30
2.6 Hydroxyproline assay.....	33
2.7 Second harmonic generation.....	34
2.8 Adult cardiac fibroblast isolation and culture.....	36
2.9 Statistical analysis.....	38
Chapter 3. Results	39
3.1 Loss of ADAM15 impairs recovery from myocardial infarction...40	40
3.2 Impact of ADAM15-deficiency in inflammatory response following myocardial infarction.....46	46
3.3 Absence of ADAM15 markedly impairs collagen fiber organization and assembly.....49	49
3.4 Reduced fibronectin content in the ADAM15-deficient infarcted myocardium.....53	53
3.5 In adult cardiac fibroblasts lacking ADAM15, activation in response to ischemia is suppressed.....56	56
3.6 ADAM15 initiates activation of PAK1 and induces expression of fibronectin and LOX1 <i>in vivo</i> and <i>in vitro</i>59	59
Chapter 4. Discussion	61
4.1 Discussion.....	62

4.2 The rupture rate of ADAM15 ^{-/-} mice is not the result of an altered inflammatory response.....	62
4.3 ADAM15 plays a role in the fibrotic response to MI.....	64
Chapter 5. Limitations and future directions.....	68
5.1 Limitations.....	69
5.1.1 Disease model for heart failure.....	69
5.1.2 Ischemia models <i>in vitro</i>	69
5.2 Future directions.....	71
5.2.1 Role of ADAM15 in an ischemia reperfusion model.....	71
5.2.2 Elucidate sex differences in ADAM15-deficient mice.....	71
References	74

List of Tables

Table 2.1 Mouse assay IDs for TaqMan real-time PCR.....	33
Table 3.1 Echocardiographic assessment of heart function in WT and <i>Adam15</i> ^{-/-} mice and corresponding shams at 3 days and 1-week post-MI.....	46

List of Figures

Figure 1. Schematic of integrin, fibronectin and collagen interactions.....	17
Figure 2. Structure of ADAMs.....	20
Figure 3. Absence of ADAM15 leads to left ventricular rupture.....	42
Figure 4. Loss of ADAM15 impairs contraction of the posterior base segment.....	44
Figure 5. Absence of ADAM15 does not affect the inflammatory response post-MI.....	49
Figure 6. Absence of ADAM15 attenuates fibrotic response to MI.....	52
Figure 7. ADAM15-deficient mice have reduced fibronectin expression and secretion.....	55
Figure 8. Presence of ADAM15 promotes activation of fibroblasts.....	58
Figure 9. ADAM15 interacts with PAK1.....	60
Figure 10. Schematic representation of ADAM15 interaction with PAK1 and PAK1 regulation of fibronectin via PAK1-NF-kB-p65.....	67
Figure 11. Loss of ADAM15 in female mice does not alter LOX-1 upregulation post-MI as compared to the female WT counterpart.....	73

List of Abbreviations

A'	Tissue Doppler velocity due to atrial contraction
A'/E'	Ratio of A' to E'
A-wave	Transmitral inflow velocity due to atrial contraction
ACUC	Animal Care and Use Committee
ADAM	A disintegrin and metalloproteinase
<i>Adam15</i> ^{-/-}	A disintegrin and metalloproteinase 15 deficient
AOTF	Acousto-Optic tunable filter
α SMA	Alpha smooth muscle actin
ATP	Adenosine triphosphate
AV	Atrioventricular
Ca ²⁺	Calcium ion
CaCl ₂	Calcium chloride
CCL2	Chemokine (C-C motif) ligand 2
CCL3	Chemokine (C-C motif) ligand 3
CCL5	Chemokine (C-C motif) ligand 5
CCR	Chemokine (C-C motif) receptor
CD38	Cluster of differentiation 38
CD68	Cluster of differentiation 68
CD168	Cluster of differentiation 168
CD206	Cluster of differentiation 206
cFB	Cardiac fibroblast
CO	Cardiac output
COL1 α 1	Collagen type I alpha 1 chain
COL1 α 2	Collagen type I alpha 2 chain
COL3 α 1	Collagen type 3 alpha 1 chain
DAMP	Danger associated molecular pattern
DAPI	4',6-Diamidino-2-Phenylindole
DMEM	Dulbecco's modified – Eagle's Medium
DT	Deceleration time
E'	Early tissue Doppler velocity
E'/A'	Ratio of E' to A'
E-wave	Early transmitral peak velocity
E/A	Ratio of E-wave to A-wave
E/E'	Ratio of E-wave to E'
ECM	Extracellular matrix
EDTA	Ethylenediaminetetraacetic acid
EF	Ejection fraction
EGF	Epidermal growth factor
EGR2	Early growth response 2
ERK1/2	Extracellular signal-regulated protein kinase 1/2
FAC	Fractional area change
FN/FN-1	Fibronectin
FoxO4	Forkhead box protein O4
FT	Fibrinolytic therapy

GLS	Global longitudinal strain
H ₂ O	Dihydrogen monoxide
HCl	Hydrogen chloride
HELP	Human explanted heart program
HEPES	4-(2-hydroxyethyl)-1piperazineethanesulfonic acid
HOPE	Human organ procurement and exchange
HPRT	Hypoxanthine-guanine phosphoribosyltransferase
I/R	Ischemia/reperfusion
ICAM-1	Intracellular adhesion molecule 1
IL-1	Interleukin 1
IL-1R	Interleukin 1 receptor
IL-6	Interleukin 6
IL-10	Interleukin 10
IL-18	Interleukin 18
IR	Infrared
IVCT	Isovolumic contraction time
IVRT	Isovolumic relaxation time
IVS	Interventricular septum
KCl	Potassium chloride
KH ₂ PO ₄	Potassium dihydrogen phosphate
LAD	Left anterior descending
LOX-1	Lysyl oxidase 1
LV	Left ventricle
LVID	LV internal diameter
LVPW	LV posterior wall
Ly6B.2	Lymphocyte antigen 6B.2
MAPK	Mitogen-activated protein kinase
MCP-1	Monocyte chemoattractant protein 1
MEK1/2	MAPK/ERK Kinase 1/2
MgSO ₄	Magnesium sulfate
MI	Myocardial infarction
MPEF	Multiphoton excitation fluorescence
Na ⁺	Sodium ion
Na ₂ HPO ₄	Disodium phosphate
NaCl	Sodium chloride
NaHCO ₃	Sodium bicarbonate
NaOH	Sodium hydroxide
OCT	Optimal cutting temperature compound
P-PCI	Primary Percutaneous Coronary Intervention
PAK1	p21-activated kinase 1
PBS	Phosphate buffered saline
PDGF	Platelet derived growth factor
PDGFR	Platelet derived growth factor receptor
PLA	Proximity ligation assay
PVDF	Polyvinyl Difluoride
RGD	Arginine-glycine-aspartic acid

RT-PCR	Real time polymerase chain reaction
SERCA	Sarco-/Endoplasmic Reticulum Ca ²⁺ -ATPase
SH3	Src homology 3
SHG	Second harmonic generation
TGFβ	Transforming growth factor beta
TLR	Toll-like receptor
TNFα	Tumor Necrosis Factor alpha
TRPC6	Transient receptor potential cation channel subfamily C member 6
VEGF	Vascular endothelial growth factor
WMSI	Wall motion score index
WT	Wildtype
Ym1	Chitinase 3-like 3
Zn ²⁺	Zinc ion

Chapter 1

Introduction

1.1 Introduction

Cardiovascular diseases and their associated morbidities and mortalities are a major health issue worldwide, and with an aging global population the impact these diseases have on society is increasing.¹ Maintaining healthy heart function is a result of a complex interaction between cardiomyocytes and non-cardiomyocytes via the extracellular matrix (ECM). The ECM present in the heart is constituted of the fibrillar component, the basement membrane and the proteoglycans. As a result of a cardiovascular disease, such as ischemic cardiomyopathy, the heart undergoes adverse changes to the heart structure, function and cellular makeup. These microscopic and macroscopic changes contribute to the development of heart failure, ergo, a cessation or attenuation of these changes will be vital in mitigating to the damage caused by an ischemic event to the myocardium.

1.2 Anatomy of the Heart

The human heart is a muscular organ situated in a fluid filled sac called the pericardial cavity located in the thoracic cavity. The tip of the heart, known as the apex, rests above the diaphragm. The base of the heart is attached to the aorta, pulmonary artery, pulmonary vein, and vena cava. The heart is a circulatory pump which delivers deoxygenated blood from the right side of the heart to the lungs, and oxygenated blood returning from the lungs from the left side of the heart to the body via the aorta.

The heart wall consists of three muscular layers. Briefly, the pericardium is a thin covering that segregates the heart from other organs inside the thoracic cavity. The myocardium is the muscular middle layer of the heart wall responsible for heart contractions and blood flow. The endocardium is the innermost layer of tissue that lines the chambers of the heart, and is primarily made up of endothelial cells. This layer allows blood cells and platelets to flow through the heart without attaching to the heart's walls.

Four chambers make up the heart: the right atrium, right ventricle, left atrium and left ventricle. Atria are smaller in size compared to the ventricles, and passively and actively fill the ventricles with blood. The larger ventricles act to carry blood away from the heart. The right side of the heart (pulmonary circulation) is smaller than the left side of the heart (systemic circulation) due to the hemodynamic requirements placed on each side of the heart.

The cardiac cycle of diastole (relaxation of the heart) and systole (contraction of the heart) contains five phases: isovolumic relaxation, ventricular filling, atrial contraction, isovolumic contraction, and ventricular ejection.

During isovolumic relaxation, the pressure inside of the ventricles decreases as the heart relaxes. The atrioventricular valves (AV) valves and semilunar valves remain closed during this phase, preventing blood flow to the ventricles. As the pressure continues to drop the AV valves open and blood enters the ventricle passively. Following passive filling the atria contract and actively fill the ventricles. The atria relax and the next phase starts. Isovolumic contraction

begins when the heart starts to contract. As pressure builds in the ventricle the AV valves close and prevent blood flow into the ventricles. As pressure builds in the ventricles, the semilunar valves open allowing blood to leave the heart during the ventricular ejection phase. The ventricles begin to relax and the cycle restarts.

1.3 Cell types in the heart

The human heart consists of different cell types (i.e. cardiomyocytes and non-myocyte cells). Cardiomyocytes constitute 25-30% of all cells in the heart.² The non-myocyte cells consist of endothelial cells, hematopoietic-derived cells and fibroblasts. Endothelial cells represent over 60% of the cardiac non-myocyte cell population, hematopoietic-derived cells represent 5-10% and fibroblasts represent under 20%.²

The cardiomyocytes are the contracting cell of the heart and are interconnected via gap junctions which facilitate the propagation of action potentials, and excitation-contraction coupling. The sarcolemma layer, sarcoplasmic reticulum and sarcomere are integral for excitation-contraction coupling.

The sarcolemma layer is the cell membrane of the cardiomyocytes and contains ion pumps, exchangers, and transmembrane receptors. L-type calcium channels initiates excitation-contraction coupling, while $\text{Na}^+/\text{Ca}^{2+}$ exchanger transports the aforementioned ions across the cell membrane. The Ca^{2+} -ATPase system pumps the calcium ions slowly out of the cardiomyocytes into the interstitial space.

The sarcoplasmic reticulum is primary storage site for Ca^{2+} in the cardiomyocyte during contraction. The SERCA2A pump is an ATP-dependent Ca^{2+} pump that is responsible for the reuptake of intracellular Ca^{2+} and enables cardiomyocyte relaxation. Activation of ryanodine receptors occurs when voltage-gated L-type Ca^{2+} channels are activated by an action potential. This facilitates the movement of Ca^{2+} into the cardiomyocyte and combines electrical events into chemo-mechanical events. Incoming Ca^{2+} activates the ryanodine receptors creating a release of Ca^{2+} into the cytosol. Un-phosphorylated phospholamban inhibits SERCA2A and attenuates its ability to uptake cytosolic Ca^{2+} , which enables Ca^{2+} to act on sarcomere proteins, in turn facilitating chemo-mechanical events.

The sarcomere is the main contractile unit of the cardiomyocytes and contains actin, myosin, troponin complex, and tropomyosin. These proteins act in concert with Ca^{2+} to contract the cardiomyocytes.

Non-myocardial cells such as endothelial cells are found in both the myocardium and endocardium. Coronary arteries are comprised of endothelial cells and smooth muscle cells that regulate vascular tone and blood flow to the myocardium. Cardiac fibroblasts are cells that produce various ECM products, commonly collagens, which gives stability to cells found in the heart and promotes correct structural form and functionality of the heart.

1.4 Ischemic Cardiomyopathy

Cardiomyopathies are a group of diseases that negatively affect the heart and its function. Hypertrophic cardiomyopathies, dilated cardiomyopathies, and ischemic cardiomyopathies reduce heart function and may result in death.

Hypertrophic cardiomyopathy is the most common cardiomyopathy and is defined by left ventricular hypertrophy without chamber dilation.³ This can be attributed to a variety of sarcomere gene mutations and 60% of patients with hypertrophic cardiomyopathy have a familial disease.⁴ One of the most common genes affected in hypertrophic cardiomyopathy encodes myosin binding protein-C.⁵ Mutations affect the ability of myosin binding protein-C to limit cross-bridge interactions that facilitate cardiomyocyte contraction.⁶ Mutations of this protein result in augmentation of myosin contractility and cardiac hypertrophy.⁶

Dilated cardiomyopathy is characterized by ventricular chamber enlargement and systolic dysfunction. Dilated cardiomyopathy can be attributed to a variety of gene mutations involving proteins in the sarcomere, nuclear envelope, and cell membrane.⁷⁻⁹ Up to 40% of dilated cardiomyopathy may be inherited.¹⁰ In the normal heart the basement membrane interacts with fibrillar collagen and the cardiomyocyte. A key component in this interaction is the dystrophin-glycoprotein complex (DGC). In short, the DGC is made of a series of transmembrane proteins that interact with the sarcolemma of the cardiomyocyte and the extracellular milieu.¹¹ Mutations of proteins in the DGC, such as dystrophin, can

lead to dilated cardiomyopathy by impairing the formation of the DGC.^{12, 13} This results in an uncoupling of the sarcomere and the ECM, leading to increased membrane instability and cardiac remodeling. Ischemic cardiomyopathy, described below, is a multifactorial disease that is influenced by environmental factors as well as genetic factors.¹⁴

Ischemic cardiomyopathy results from damage to the myocardium due to a narrowing or blockage of the coronary arteries, which causes a reduced blood supply, nutrients and oxygen to the myocardium. In the response to this ischemic insult happening (i.e. in the LV), the LV dilates and enlarges. This reduces the pumping ability of the heart and is labelled LV remodeling. A complete blockage of a coronary artery is called a myocardial infarction (MI), or in popular vernacular a heart attack. In response to a blockage, areas downstream of the blockage begin to undergo a number of molecular and cellular events which include cell death, apoptosis, inflammation, reduced angiogenesis, eccentric cardiomyocyte growth, and fibrosis. These events combine to develop adverse LV remodeling by dilating the LV, thinning the myocardium, and the formation and expansion of the infarct. To summarize, ischemic cardiomyopathy affects overall heart morphology and pumping function and can lead to heart failure.

1.4.1 Epidemiology

Data acquired on the prevalence, incidence and all cause mortality in Canada highlights sex differences in how often and the outcome of an ischemic

event in the heart can affect different individuals. These data were extensively covered in the Report from the Canadian Chronic Disease Surveillance System: Heart Disease in Canada, 2018.¹⁵ Below is a summary of the relevant findings pertaining to this thesis.

Occurrence of a MI was higher among men than woman in Canada. As men and women age, the prevalence of a MI increases and the gap between the sexes narrows. The incidence for MI is 2.1 times higher for men than women on average, with women tending to develop heart disease 10 years later than men.^{15, 16} The difference in incidence also decreases as men and women age. This sex difference may be explained by the presence of sex hormones in pre-menopausal woman, as estrogen may have a cardioprotective effect in woman.¹⁶⁻¹⁸ The rise in post-menopausal women experiencing an ischemic event can also be explained by a decrease in estrogen.^{15, 17, 18} However, this mechanism is not fully understood. Young women with estrogen deficiency have a sevenfold increase in coronary artery risk.¹⁹ Estrogen impacts liver lipid metabolism as liver genes involved with triglyceride and cholesterol metabolism vary with estrous cycle in mice.²⁰ Estrogen can also inhibit IL-6 expression by inhibiting NFkB through the binding of estrogen receptor- α to NFkB, and by doing so can limit an inflammatory response.²¹ Estrogen may play a vital role in preventing the accumulation of cholesterol, thereby attenuating plaque formation and myocardial infarction.²²

Men diagnosed with ischemic heart disease were more likely to die of any cause than women. However, women were more likely to die of any cause after a

MI.¹⁵ This could be due to a number of causes. One such cause is misdiagnosis.²³ Women typically present with fewer typical symptoms than men, and they are more likely to present at the hospital without chest pain or having mild chest pain leading to a misdiagnosis.²⁴ Because women experience milder outward symptoms, women wait longer to seek medical care which could lead to a poorer outcome.²³

1.4.2 Risk factors

Reducing or eliminating risk factors in everyday life is beneficial for both men and women. These risk factors include: age, as having a MI increases with age;²⁵ tobacco use, including smoking and exposure to second-hand smoke;²⁶ high blood pressure, as increased blood pressure can damage arteries and if in accompaniment with other conditions (i.e. obesity, high cholesterol, or diabetes) can increase the risk of a MI even more.^{26, 27} High levels of low-density lipoprotein cholesterol and high levels of triglycerides increases the risk of a MI.^{28,}²⁹ Obesity has been linked to high cholesterol, high triglycerides, high blood pressure and diabetes.³⁰ All of which increase the risk of having a MI. A lack of response to elevated glucose levels, as seen in diabetes, increases MI risk.³¹ Metabolic syndrome occurs in response to obesity, high blood pressure and high blood sugar, and increases the chances of developing heart disease twice as likely compared to a person without metabolic syndrome.³² A lack of physical activity, stress, and illicit drug use all increase the chance of a MI. Genetics also play a role, as people related to individual who had an early MI (before age 55 for

men and 65 for women) are more likely to also have a MI.³³ Women with a history of preeclampsia are more vulnerable as well.³⁴ Autoimmune diseases such as rheumatoid arthritis or lupus also increase the risk of a MI.^{35, 36}

1.4.3 Pathogenesis

Cardiac repair post-MI results from a complex series of events, beginning with an inflammatory response that digests and clears the damaged cells and ECM from the infarcted area. This is followed by a reparative phase with the resolution of inflammation, the proliferation of myofibroblasts, fibrosis and scar formation, and neovascularization. Early inflammation is required for necessary wound healing. Appropriate and timely resolution of inflammation can determine how successful the wound healing can be. An excessive inflammatory response can augment the deleterious effects brought about by the infiltration of inflammatory cells, such as improper scar formation, and infarct expansion leading to adverse remodeling and chamber dilation.

As a result of an ischemic event in the LV, myocardium downstream of the blockage are not perfused with oxygenated blood resulting in a hypoxic environment. Hypoxia impairs vascular endothelial permeability, which facilitates the infiltration of leukocytes.³⁷ In response to prolonged ischemia (lack of nutrients and oxygen), cell necrosis begins.³⁷ Necrotic and damaged cells, including cardiomyocytes and damaged ECM, release danger-associated molecular patterns (DAMPs) that act on the innate immune system on surviving

resident macrophages and infiltrating leukocytes.^{38, 39} This robustly activates a cascade of inflammatory mediators.

Pro-inflammatory cytokines such as IL-1, TNF α , IL-6, and IL-18 are secreted early after MI and are key propagators of the inflammatory response.⁴⁰⁻⁴³ These cytokines act to amplify the inflammatory response by activating the NF κ B inflammatory pathways.⁴⁴⁻⁴⁶ They also create a local paracrine milieu of pro-inflammatory molecules that can act on present and infiltrating cells.⁴⁷ They also serve in the recruitment of leukocytes by upregulating adhesion molecules to facilitate infiltration.⁴⁸ *Il-1r*-deficient mice and wild-type mice treated with anti-TNF antibodies exhibit smaller infarcts, reduced leukocyte infiltration, and lower expression of adhesion molecules.^{49, 50} Inhibition of CCL2 (another pro-inflammatory chemokine), or *Ccl2*-deficient mice or mice deficient in CCR2 (a receptor for CCL2) also have reduced infarct size and inflammatory cell infiltration.⁵¹⁻⁵⁴

Cardiomyocytes provide the stimulus for post-MI inflammatory reaction. As stated above, necrotic cardiomyocytes produce DAMPs in the infarcted area. However, surviving cardiomyocytes surrounding the infarcted area also promote inflammation by secreting pro-inflammatory cytokines and adhesion molecules in response to IL-1 and TLR ligands (i.e. DAMPs).⁵⁵⁻⁵⁷

Endothelial cell activation of transcription factor forkhead box O4 (FoxO4) after infarction promotes neutrophil infiltration into the infarcted heart.⁵⁸ DAMPs induce upregulation of adhesion molecules, such as P- and E-selectin in

endothelial cells.⁵⁹⁻⁶¹ Once expressed, these adhesion molecules bind to their leukocyte ligands to promote adhesion and mediate rolling along the endothelium.⁶² Activated endothelial cells are also a source of cytokines and chemokines.^{63, 64}

Neutrophils are the first inflammatory cell to infiltrate the infarcted region in response to the abundance of DAMPs, cytokines and chemokines, and adhesion molecules.⁶⁵⁻⁶⁸ Activated neutrophils express ligands for the selectins and bind to the activated endothelial cells to enable infiltration.⁶⁹ Extravasation requires the binding of leukocyte integrins and endothelial adhesion molecules, and adhesion molecules with junctional proteins.⁷⁰⁻⁷³ Upon infiltration into the infarcted region, neutrophils release proteolytic enzymes and contribute to wound clearance by digesting dead cells and ECM debris.⁷⁴ Neutrophils can also extend the inflammatory response and augment the ischemic injury by cytotoxic actions on viable cardiomyocytes.⁷⁵⁻⁷⁷

Monocytes are also recruited in a similar way to neutrophils. Pro-inflammatory monocytes are recruited via the CCL2/CCR2 axis.⁵² These activated M1 macrophages are pro-inflammatory, anti-fibrotic, and anti-angiogenic. These macrophages work to clear the wound of debris, and can originate from bone marrow, as well as the spleen.⁷⁸ Resident macrophages play a protective role post-MI. Deletion of resident macrophages resulted in impaired cardiac function and promoted adverse remodeling post-MI, which highlights a non-redundant, cardioprotective role.⁷⁹

Fibroblasts can also be stimulated by DAMPs, reactive oxygen species and IL-1.^{80, 81} In response to this activation, fibroblasts gain a pro-inflammatory phenotype and secrete cytokines and chemokines. IL-1 signaling in fibroblasts inhibits α -smooth muscle actin (α SMA) expression, which impedes the transformation of fibroblasts into myofibroblasts.⁸¹ This pathway may prevent a premature activation of myofibroblasts, and an early fibrotic response that could be damaged by the presence of neutrophils and macrophages or impeded by dead cells and debris.

As both cardiomyocytes and non-cardiomyocytes are surrounded by ECM proteins, damage to the ECM also activates the inflammatory response. Collagen and fibronectin fragments are implicated in the activation and recruitment of inflammatory cells.⁸²⁻⁸⁴

Neutrophils are typically short-lived cells that undergo cell death primarily via apoptosis.^{66, 85} Late-stage apoptotic neutrophils promote inflammation resolution by the release of mediators that attenuate neutrophil transmigration and entry, and promote neutrophil apoptosis and digestion by macrophages.^{66-68, 85} Apoptotic neutrophils also express scavenger receptors for cytokines and chemokines to facilitate tissue depletion of these molecules.⁴³⁻⁴⁵ Apoptotic neutrophils also express signals that attract digestion by macrophages.⁴³⁻⁴⁵

This phagocytic activity by macrophages on apoptotic neutrophils facilitates a phenotypic switch in macrophages from a M1 phenotype that is pro-inflammatory to a M2 phenotype that is anti-inflammatory and pro-fibrotic.⁸⁶ M2

macrophages secrete IL-10, an anti-inflammatory cytokine, and transforming growth factor- β (TGF- β).^{87, 88} TGF- β suppresses inflammation and promotes tissue repair and fibrosis.^{89, 90} M2 macrophages promote angiogenesis via increased expression of vascular endothelial growth factor (VEGF).⁹¹⁻⁹³

Tissue neovascularization resupplies the infarcted zone with oxygen and nutrients which is crucial for wound healing post-MI. This occurs during the inflammatory response as well as contributes to the resolution of inflammation. Newly formed blood vessels lack a pericyte and smooth muscle cell layer.^{94, 95} This serves to promote hyperpermeability of the vessels and promotes extravasation into the infarcted area. However, during the later stages of infarct healing the blood vessels mature and gain the pericyte and smooth muscle cell layer. Platelet derived growth factor (PDGF) acts on its receptor PDGFR β on both pericytes and smooth muscle cells to accomplish this.⁹⁵ Attenuation of this process results in prolonged inflammation and poorer infarct healing. The importance of pericytes is highlighted by the effects of pericyte transplantation. Human pericyte transplantation into the peri-infarcted zone of mice reduces vascular permeability and leukocyte infiltration, promotes angiogenesis and improves LV remodeling.^{96, 97}

Upon resolution of inflammation, collagen is deposited by myofibroblasts to form the scar. Myofibroblasts are fibroblasts that develop stress fibers and express contractile proteins such as α SMA, and this cellular change mark the start of the proliferative phase of cardiac repair.⁹⁸⁻¹⁰¹ Myofibroblasts can originate from resident quiescent fibroblasts that originated in the heart or they could

originate from circulating bone marrow progenitors.^{102, 103} Another source of myofibroblasts is from mesenchymal transdifferentiation, in which endothelial cells and pericytes transform into myofibroblasts.^{104, 105} In summary, fibroblasts that survive the ischemic environment and cells recruited from the surrounding tissue can transdifferentiate into myofibroblasts in response to bioactive TGF β .

Myofibroblast conversion is dependent on a number of factors. TGF β -mediated myofibroblast conversion of fibroblasts requires an outside-in signal from fibronectin.^{106, 107} Transient receptor potential C6 (TRPC6), an ion channel, is critical for myofibroblast differentiation.¹⁰⁸ Absence of TRPC6 is associated with attenuated fibroblast function and increased cardiac rupture.¹⁰⁹

Following myofibroblast activation, the myofibroblasts produce ECM proteins starting from the peri-infarcted area and progress to the core infarct area along the newly synthesized ECM matrix.¹¹⁰ Myofibroblasts produce large amounts of collagen which is crucial for increasing tensile strength and preventing ventricular rupture. Myofibroblasts also secrete fibronectin and various other matricellular proteins to promote myofibroblast migration and recruitment for wound healing.¹¹¹ Collagen fibers are cross-linked by lysyl oxidase, and cross-linking is a requirement for the tensile strength of the scar.¹¹² Fibronectin also promotes activation of lysyl oxidase.¹¹³ As the new collagen-based ECM is established, pro-fibrotic growth factors and matricellular proteins are depleted.⁸⁰ In turn, this leads to the partial removal of myofibroblasts from the infarcted area.

Unfortunately, the cardiac remodeling that occurs post-MI causes deleterious long-term effects on the heart during the maturation phase of cardiac wound healing. Due to the fibroblast-mediated expansion of the ECM, surviving cardiomyocytes undergo hypertrophy to compensate for the increased workload.¹¹⁴ Excessive cross-linked collagen attenuates the diastolic function of the heart leading to heart failure.¹¹⁵ Because of the compromised function of the hypertrophic cardiomyocytes in the non-infarcted region, mechanical stress is increased and latent TGF β is activated.⁸⁰ This mechanism promotes fibrosis in the non-infarcted region and further impediment of the surviving cardiomyocytes. As more surviving cardiomyocytes die, they are replaced with collagen which further impairs the surrounding cardiomyocytes causing more cell death. In turn, the infarcted area expands beyond what was initially damaged by the ischemic event. This cycle repeats itself indefinitely as activated myofibroblasts are found in the hearts of MI patients' years after the initial ischemic insult.^{80, 116}

The role of fibronectin in post-MI wound healing cannot be understated. Fibronectin is a protein found in a subcategory of the extracellular matrix called the basement membrane. The basement membrane serves as the interface between cardiomyocytes and other cells and the interstitial ECM.¹¹⁷ Fibronectin plays a role in this process by binding to cell surface receptors and other ECM proteins such as collagens (Figure 1). Fibronectin (FN) is produced by a variety of cardiac cell-types and as stated before, promotes myofibroblast transformation. Fibroblasts attach to FN via integrin $\alpha_4\beta_7$, and blocking this interaction limits the ability of fibroblasts to adhere to fibronectin.¹¹⁸ The action of

fibroblast adherence to fibronectin promotes myofibroblast differentiation through the MAPK-ERK1/2 pathway.¹¹⁸ Inhibition of MEK1/2 inhibited fibronectin induced α SMA expression.¹¹⁹ TGF β is unable to cause myofibroblast differentiation by itself and requires fibroblast adherence to fibronectin.¹²⁰ FN deposition is increased in the infarcted area following a MI.¹²¹ Inhibition of FN polymerization attenuated myofibroblast activation and limited the resulting fibrotic deposition.¹²² The transition of fibroblasts to myofibroblasts and the cross-linking of collagen is mediated by fibronectin.

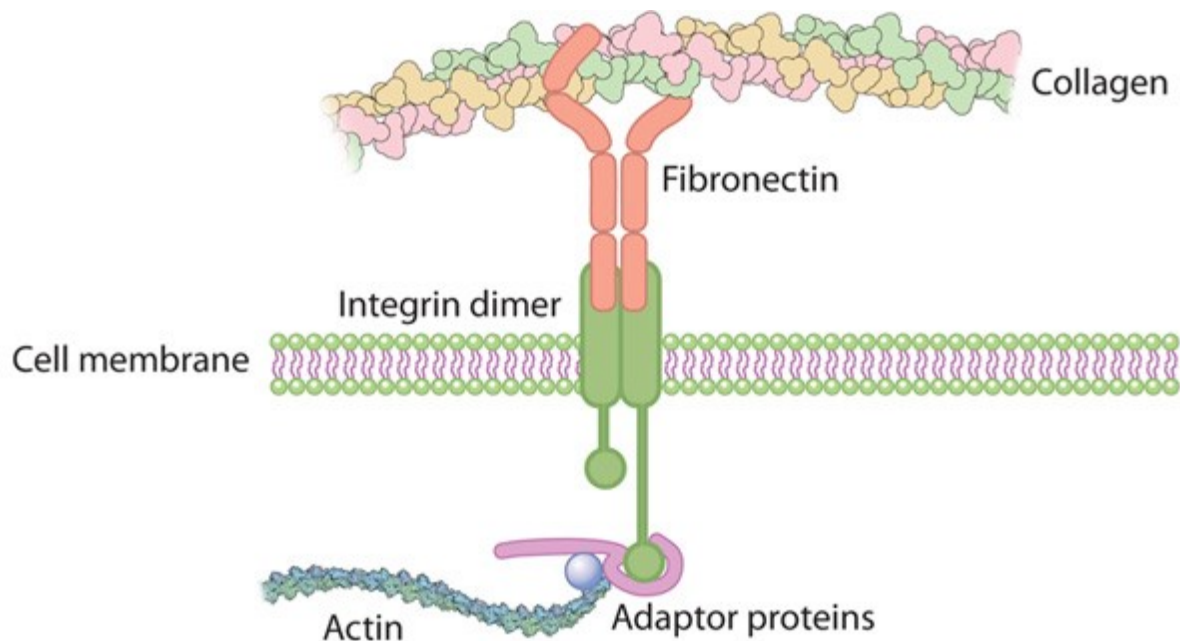


Figure 1. Schematic of integrin, fibronectin and collagen interactions.

Illustration of how fibronectin facilitates the interactions between collagen and the cell. Adapted from Nature Education, 2010.¹²³

1.4.4 Treatment of MI

Initial treatment of a MI involves coronary reperfusion strategies that focus on removing the blockage and resupplying the ischemic area with blood. This is

done by fibrinolytic therapy (FT) and Primary Percutaneous Coronary Intervention (P-PCI), with P-PCI being superior. However, delays in door-to-balloon time are associated with increased mortality so the timely administration of some form of reperfusion therapy is optimal.¹²⁴⁻¹²⁷ Administration of pre-hospital FT results in reduced mortality, and immediate FT may be advantageous even if the wait time for P-PCI is short.¹²⁸⁻¹³⁰ Dual antiplatelet therapy should be administered prior to FT, and continue for at least 1-year post-MI regardless of reperfusion technique.^{131, 132} Anticoagulants are also used in both the short and long term of MI patients.¹³³

P-PCI administration in a timely manner is superior to FT and has lower rates of post-intervention complications such as recurrent ischemia, reinfarction, emergency repeat revascularization procedures, and death.^{134, 135} A phenomenon called “no reflow” can occur where myocardial perfusion is inadequate for the heart tissue after the blockage has been removed.¹³⁶ This can occur as a result of a combination of factors such as endothelial injury, edema, vasospasm, myocyte reperfusion injury and inflammation.¹³⁶ Compared to balloon angioplasty, metal stents have been shown to reduce the rates of reinfarction; however, this has not reduced mortality.¹³⁷ Drug eluting stents reduce the need for reintervention and it significantly reduced the rate of restenosis and stent thrombosis.¹³⁸⁻¹⁴⁰

1.5 Disintegrin and Metalloproteinases: ADAMs

A disintegrin and metalloproteinases (ADAMs) are Zn^{2+} -dependent transmembrane proteins with homology to the adamalysin metalloproteinase family, a group of proteins found in snake venom that act as integrin ligands.¹⁴¹ The ADAMs family share a highly conserved structural homology and are composed of a N-terminal pro-domain followed by a metalloproteinase domain, a disintegrin domain, a cysteine-rich region, an EGF-like domain, a transmembrane domain, and a C-terminal cytoplasmic tail (Figure 2).

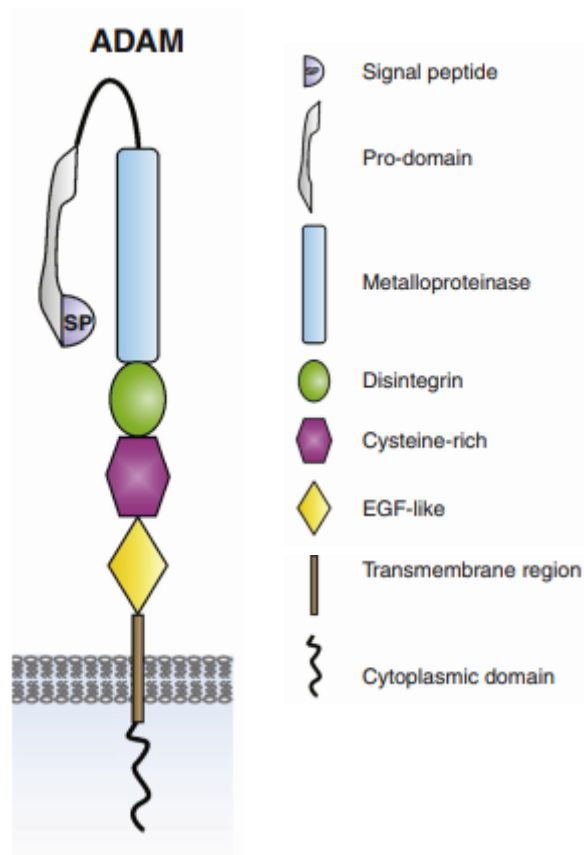


Figure 2. Structure of ADAMs. Linear structure and domain organization in ADAMs (a disintegrin and metalloproteinase). Adapted and used with permission from Chute *et al.* 2018.¹⁴²

1.5.1 Pro-domain

The N-terminal pro-domain contains a signal peptide and a pro-domain. The pro-domain functions to keep its respective ADAM in a catalytically inactive state, by physically blocking the metalloproteinase catalytic site. This is accomplished by a cysteine-switch mechanism, in which a cysteine residue in the pro-domain forms a complex with Zn²⁺ in the metalloproteinase domain.^{141, 143, 144} The pro-domain ensures proper protein folding prior to entry into the secretory pathway, and prevents protein degradation during transport through the secretory pathway.¹⁴⁵ Pro-domains that have been synthesized or purified can act as potent inhibitors of their respective active ADAMs.^{146, 147}

The signal peptide directs intracellular trafficking of an ADAM from the endoplasmic reticulum to the late Golgi.¹⁴⁸ Here the pro-domain is proteolytically cleaved by furin-like proprotein convertases.¹⁴⁸

1.5.2 Metalloproteinase

Attached to the pro-domain is the metalloproteinase domain. Humans have 20 functional ADAMs with 12 of them being catalytically active (i.e. ADAMs 8-10, 12, 15, 17, 19-21, 28, 30, and 33).¹⁴¹ Mice, however, have 17 proteolytically active ADAMs.¹⁴¹ Through the use of cell-based shedding experiments, *in vitro*

cleavage assays, or genetic models have elucidated the degradome for ADAMs.¹⁴⁹ The cleavable substrates for ADAMs include growth factors, cytokines and/or their receptors, and cell adhesion molecules.¹⁴¹ Substrates for ADAMs also include soluble proteins like insulin-like growth factor-binding proteins 3 and 5, or are a part of the ECM like collagen IV and fibronectin.^{150, 151}

1.5.3 Disintegrin domain

Downstream of the metalloproteinase domain is the disintegrin domain. The disintegrin domain enables ADAMs to interact with integrins via a disintegrin loop.¹⁵² ADAMs can interact with various integrins through the disintegrin loop, and the different residues within the loop interact with different integrins.^{153, 154} This action enables the regulation of cell adhesion, cytoskeleton reorganization and cell polarity.¹⁵⁵ In human ADAM15, a RGD sequence is present in the disintegrin domain.¹⁵⁶ The RGD sequence is also found in snake venom disintegrins and may aid in integrin binding. Other ADAMs, including mouse ADAM15, do not contain this sequence and may limit the number of integrins that can be bound.¹⁵⁶

1.5.4 Cysteine-rich region

All ADAMs contain a cysteine-rich region and this region may affect ADAM function. ADAM12, for instance, interacts with syndecans through the cysteine-rich region.¹⁵⁷ This interaction enables further engagement to β_1 -containing integrins.¹⁵⁷ ADAM13 interacts with fibronectin through the disintegrin/cysteine-

rich domains.¹⁵⁸ It was also found through domain deletion analysis that ADAM17 requires the cysteine-rich region to shed IL-1 Receptor-II but not for its ability to shed TNFa.¹⁵⁹ These findings, among others, suggest that the cysteine-rich region is important for biological functions such as integrin-binding, cell adhesion, and protease activity.

1.5.5 EGF-like domain

Most ADAMs, excluding ADAM10 and ADAM17, have an EGF-like domain.¹⁶⁰ This domain is placed between the cysteine-rich domain and the transmembrane domain. Though the exact mechanism of action is unknown, it is thought that this domain acts to conform the shape of ADAMs into a C-shaped arm composed of the metalloproteinase domain, the disintegrin domain and the cysteine-rich domain.¹⁶¹ This structure may enable substrate recognition by allowing individual domains to interact with the same protein.

1.5.6 Cytoplasmic tail

The cytoplasmic tails of ADAMs differ in terms of lengths and composition. Many cytoplasmic tails contain a Src homology 3 domain (SH3) binding sites or sites for phosphorylation.¹⁴¹ Binding partners to the cytoplasmic tail affect protease activity, intracellular transport, localization and cell signalling. A detailed list of binding partners for ADAM9, ADAM10, ADAM12, ADAM13, ADAM15, ADAM17 and ADAM22 has been previously documented.¹⁴¹ Phosphorylation of the cytoplasmic tail could regulate maturation, trafficking, membrane localization

and proteolytic activity of ADAMs. Cytoplasmic domain variants of ADAM15 in breast cancer indicate isoform specific associations with clinical outcome as well as effects on cell adhesion and migration.¹⁶²

1.6 ADAM15

The particular ADAM that is being focused on for the following research is ADAM15 due to the ability of ADAM15 to impact transendothelial migration.¹⁶³ ADAM15 was first found to be expressed in human endothelial cells and then subsequently in animal vasculature.^{164, 165} It was found to have increased expression in the heart following MI.¹⁶⁶ During atrial fibrillation, ADAM15 expression was increased compared to during sinus rhythm in the human heart.¹⁶⁷ ADAM15 has been linked to a endothelial permeability as overexpression of ADAM15 in human umbilical vein endothelial cell monolayers facilitated transendothelial migration of neutrophils.¹⁶⁸ It was also involved in a vascular endothelial growth factor amplification loop that promoted ocular neovascularization.¹⁶⁹ ADAM15 has also been linked to atherosclerosis by impairing endothelial permeability, and facilitating neutrophil and monocyte infiltration.¹⁶³ ADAM15 has also been involved in vascular leakage during sepsis.¹⁷⁰

1.7 Rationale

Although ADAM15 is involved in numerous processes that occur during a MI such as inflammation, this is the first attempt to study the role of ADAM15 in

ventricular remodeling following a MI. ADAM15 has been implicated in augmenting endothelial permeability, and this mechanism may play a role in post-MI remodeling by limiting the infiltration of inflammatory cells into the infarcted region.^{163, 168}

1.8 Hypothesis

Absence of ADAM15 will preserve endothelial barrier and reduce the inflammatory response to an ischemic insult, and therefore be beneficial for post-MI remodeling by reducing infarct expansion.

1.9 Objectives

Objective 1: To characterize the functional and structural changes in *Adam15*^{-/-} mice post-MI.

Objective 2: To determine the role ADAM15 plays in affecting transmigration and leukocyte phenotypes.

Objective 3: To identify the role ADAM15 plays in collagen deposition and scar formation.

Objective 4: To determine the effect ADAM15 deletion has on fibroblast function.

Objective 5: Identify a possible mechanism by which ADAM15 acts in a post-MI heart.

Chapter 2

Materials and Methods

2.1 Animals and surgical procedure

Myocardial infarction (MI) was induced in 11-13 week old male C57BL/6 (Wild-type; WT), and A disintegrin and metalloproteinase-15 deficient mice (*Adam15*^{-/-})¹⁶⁵. *Adam15*^{-/-} were purchased from Carl P. Blobel and bred in Health Sciences Laboratory Animal Services facilities at the University of Alberta.¹⁶⁵ Mice were anesthetized and intubated prior to surgery by Dr. Faqi Wang, a technician in the Kassiri Lab. Mice underwent a left thoracotomy in the fifth intercostal space. The pericardium was opened to expose the LV and the LAD was ligated under the tip of the left atrial appendage. Muscle and skin was closed in layers with the use of a 6-0 silk suture. Parallel sham-operated mice from each genotype served as controls. Heart function was assessed by echocardiography and speckle-tracking strain analysis at 3-day and 1-week post-MI/sham as before.¹⁷¹ Hearts were excised, flash-frozen in OCT medium, fixed in 10% formalin and processed for immunohistochemical analyses, or separated into infarct, peri- and non-infarcted regions and flash frozen for molecular analyses. All experiments were conducted in accordance with the guidelines of the University of Alberta Animal Care and Use Committee (ACUC) and the Canadian Council of Animal Care.

2.2 Human explanted heart tissue

Cardiac tissues from patients with post-MI heart failure were collected from the explanted hearts at the time of cardiac transplantation as part of the Human Explanted Heart Program (HELP) at the Mazankowski Alberta Heart Institute (Edmonton, AB). Non-failing control hearts were obtained through the Human

Organ Procurement and Exchange (HOPE) program (Edmonton, AB). All experiments were performed in accordance with the institutional guidelines and were approved by Institutional Ethic Committee. Informed consent was obtained from all subjects.

2.3 Echocardiography and strain assessments

Cardiac structure and systolic function were determined by noninvasive transthoracic echocardiography in anesthetized mice (0.75-1% isoflurane). Mice were placed on a heating pad while anesthetized, and mouse temperature and heart rate was constantly monitored during imaging. Ultrasound gel was applied to the chest, and the ultrasound probe was placed in contact with the ultrasound gel and scanning was performed over 30 minutes. Images were obtained through the use of a 30-MHz transducer (RMV-707B, Visual Sonics, Toronto, ON Canada) in conjunction with the Vevo 3100 imaging system (Visual Sonics, Toronto, ON Canada) Modified parasternal long axis EKV loops were also used to measure ejection fraction (EF) by Simpson's method. M-mode images were used to measure left ventricular (LV) chamber sizes and wall thicknesses. Fractional area change (FAC), a measure of LV global systolic function, was measured by two-dimensional echocardiography in the apical four-chamber view by measuring the functional change in the area described by the LV endocardium at peak diastole and peak systole.¹⁷¹ The wall motion score index (WMSI) was calculated based on the *American Society of Echocardiography* recommended assessment of wall motion function.¹⁷² An increase in WMSI (>1) indicates

suppressed LV systolic wall motion. Strain analysis was performed using a speckle-tracking software (Vevo Strain Analysis Software). Hearts were manually traced and the software automatically calculated global longitudinal strain as well as segment specific longitudinal strain. These segments were defined as the posterior (apex, mid, base) and anterior (apex, mid, base).

2.4 Histochemical and immunostaining analysis

For histological analyses, freshly excised hearts were arrested in diastole in 1M KCl, fixed in 10% formalin and paraffin-embedded. Trichrome staining was used to identify morphological changes at 3 days and 1-week post-MI. Masson Trichrome staining was stained at the Alberta Diabetes Institute, Histology Core, University of Alberta, Edmonton, AB, Canada. All images were captured with a Leica DM4000B microscope using Infinity Capture Software (Lumenera, Ottawa, ON, Canada).

Hearts excised 3-days post-MI were arrested in KCl, frozen in OCT medium, and sectioned using a microtome to 5 μm thick before being placed on a glass slide. stained for neutrophils (Ly-6B.2, AbD Serotec, MCA771GA), macrophages (CD68, AbD Serotec, MCA1975GA), fibronectin (Abcam, ab2413) and fibroblasts to detect inflammation and fibrosis. Cultured adult cFBs (cardiac fibroblasts) were fixed at the experimental endpoints, and stained for alpha-smooth muscle actin (Abcam, ab5694) to determine differences in fibroblast activation. Cells and heart sections were fixed in 4% paraformaldehyde, washed with PBS, permeabilized

with 0.1% Triton X-100 and incubated with 4% bovine serum albumin for non-specific blocking. Antibodies were then added to sections and cells and incubated overnight at 4°C. Sections were then washed with PBS (3 x 5 minutes) and incubated with fluorescent secondary Cy3 antibody at 37°C for 1 hour. Sections were washed and mounted with Prolong Gold antifade mounting medium containing DAPI (Life Technologies). The sections were imaged using a fluorescent microscope and Metamorph Basic software (version 7.7.0.0) and quantification was completed using the same software.

The Duolink Proximity Ligation Assay (PLA, Sigma Aldrich, DUO92105) was used to identify proteins that are less than 40 nm apart (signifying an interaction) and was completed using the manufacturer's protocol. ADAM15 (Kerafast, EHS005) and p21-activated kinase-1 (PAK1, MyBioSource, MBS420711) were used as primary antibodies. OCT frozen heart sections from WT and *Adam15*^{-/-} were fixed in 4% paraformaldehyde for 20 minutes and washed with PBS for 3 x 5 minutes. The sections were permeabilized with 0.1% Triton X-100 for 5 minutes and blocked with Duolink blocking solution and incubated for 30 minutes at 37°C. The primary antibodies listed above were added to the sections and incubated overnight at 4°C. Sections were washed with Duolink II Wash Buffer A (2 x 5 minutes). The PLA probes were diluted to the manufacturer's specifications and were added to sections to be incubated at 37°C. Sections were then washed with Wash Buffer A (2 x 5 minutes) and incubated with the ligase-ligation solution (prepared as per the manufacturer's instruction) for 30 minutes at 37°C. The

amplification solution was added to the sections and incubated at 37°C for 100 minutes. The sections were washed with Duolink Wash Buffer B for 10 minutes and mounted with Duolink II mounting medium and DAPI. Images were taken in the same manner as the aforementioned immunofluorescent imaging.

2.5 Protein and mRNA extraction and analysis

Flash-frozen hearts were segmented into infarcted, peri-infarcted, or non-infarcted regions in MI hearts and used for protein and RNA extraction. Total protein was extracted from frozen tissues using Sigma Extraction Buffer (CellLytic, C2978) with protease inhibitors (Calbiochem, 539134, 524628) and phosphatase inhibitor cocktails (Sigma Aldrich, P5726) using a mechanical lyser. Samples were centrifuged at 14,000g for 15 minutes and total protein containing supernatant was then transferred to a new tube. Total protein concentration was determine using Bio-Rad DC protein assay using a clear flat bottom 96-well plate and spectrophotometric plate reader at 750 nm. SDS based electrophoresis was used to run protein samples and for transfer of loaded protein from gel to polyvinylidene fluoride (PVDF) membrane. The appropriate amount of protein concentration was prepared by combining the calculated volume of protein extract, PBS and loading dye buffer and boiled for 5 minutes. After running the SDS gel, proteins were then transferred to the PVDF membrane at 250 mA for 2 hours at 4°C. Membranes were blocked with 3% BSA for 2 hours at room temperature. Primary antibodies (ADAM15, Kerfast, EHS005; ADAM15, R&D Systems, MAB945-SP; LOX-1, Abcam, ab31238; Fibronectin, Abcam, ab2413;

PAK1, Cell Signaling Technology, 2602S) were then added to the membrane overnight at 4°C at concentrations ranging from 1:1000 to 1:2000 in 3% BSA. The membranes were washed with Tris-buffered saline with 0.1% Tween, followed by incubation with the appropriate species based horse radish peroxidase-linked secondary antibody at room temperature for 1 hour. Membranes were then washed with the tris-buffered saline with 0.1% Tween, and Enhanced Chemiluminescence (ECL Prime, GE Amersham, Baie d'Urfe, QC Canada) was added to the membrane. The PVDF membrane was imaged using a luminescent image analyzer with a chemiluminescence-sensitive camera (GE Image Quant 4000, GE). The PVDF membrane was then stripped with a stripping buffer for 20 minutes at room temperature for subsequent immunoblotting of the membrane. Membranes were stained with a membrane stain (memcode, Thermofischer, 24580) and used as loading control. Band intensity was quantified using ImageQuant TL software (Version 7.0, GE healthcare) and normalized to loading control.

Total RNA was extracted using TRIzol Reagent (Life Technologies) according to the manufacturer's protocol and TaqMan RT-PCR was used for quantification as before.¹⁷¹ Tissue samples were homogenized in 500 µL of TRIzol in RNAase free centrifuge tubes in a tissue lyser (Qiagen, Germany, 85300), followed by centrifugation at 12,000 x g at 4°C for 10 minutes. The supernatant was transferred to another RNAase free tube and 200 µL of chloroform was added. The tubes were shaken vigorously for 10 seconds, incubated at room

temperature for 3 minutes and centrifuged at 12,000 x *g* at 4°C for 15 minutes. The upper colorless aqueous phase containing RNA was transferred to an RNAase free tube and 500 µL of isopropanol was added prior to overnight incubation at -20°C. The samples were then centrifuged at 12,000 x *g* at 4°C for 10 minutes and the supernatant was discarded. The pellet was washed with 75% ethanol and then the tubes were centrifuged at 7,500 x *g* at 4°C for 5 minutes. The supernatant was removed, the pellet was air-dried for 10 minutes and then dissolved in 20 µL of RNAase free water for quantification using the Nanodrop 1000 spectrophotometer (Nanodrop, Wilmington, DE, USA). Reverse transcription was performed on RNA samples to generate complementary DNA (cDNA). For each gene, mouse brain cDNA samples were used to generate a standard curve of known concentrations. TaqMan primer/probe cocktails were purchased from Life Technologies Corporation. Hypoxanthine-guanine phosphoribosyltransferase (HPRT) and 18S (Ribosomal RNA) was used as an internal control.¹⁷³ TaqMan assay ID for all genes are listed in Table 2.1. All values were expressed as relative expression (R.E) and samples were run in triplicate in 384-well plates.

Table 2.1 Mouse assay IDs for TaqMan real-time PCR

Gene Name	Protein Name	Assay ID
<i>Adam9</i>	A disintegrin and metalloproteinase 9	Mm01218460_m1
<i>Adam10</i>	A disintegrin and metalloproteinase 10	Mm00545742_m1
<i>Adam12</i>	A disintegrin and metalloproteinase 12	Mm00475719_m1
<i>Adam15</i>	A disintegrin and metalloproteinase 15	Mm00477328_m1
<i>Adam17</i>	A disintegrin and metalloproteinase 17	Mm00456428_m1
<i>Ccl3</i>	Chemokine (C-C motif) ligand 3	Mm00441259_g1
<i>Ccl5</i>	Chemokine (C-C motif) ligand 5	Mm01302428_m1
<i>Cd38</i>	Cluster of differentiation 38	Mm01220906_m1
<i>Cd168</i>	Cluster of differentiation 168	Mm00469183_m1
<i>Cd206</i>	Cluster of differentiation 206	Mm01329362_m1
<i>Col1a1</i>	Collagen type I alpha 1 chain	Mm00801666_g1
<i>Col1a2</i>	Collagen type I alpha 2 chain	Mm00483888_m1
<i>Col3a1</i>	Collagen type 3 alpha 1 chain	Mm00802300_m1
<i>Egr2</i>	Early growth response protein 2	Mm00456650_m1
<i>Fn-1</i>	Fibronectin	Mm01256742_m1
<i>Hprt</i>	Hypoxanthine-guanine phosphoribosyltransferase	Mm03024075_m1
<i>Il-1β</i>	Interleukin 1 beta	Mm00434228_m1
<i>Il-6</i>	Interleukin 6	Mm00446190_m1
<i>Lox-1</i>	Lysyl oxidase 1	Mm00495386_m1
<i>Mcp-1</i>	Monocyte chemoattractant protein 1	Mm00441242_m1
<i>Tnfa</i>	Tumor necrosis factor alpha	Mm00443258_m1
<i>Ym1</i>	Chitinase 3-like 3	Mm00657889_mH
α <i>Sma</i>	Alpha smooth muscle actin	Mm01546133_m1

2.6 Hydroxyproline assay

Frozen LV tissue was lyophilized, weighed (dry weight), pulverized, resuspended in 1M NaCl with protease and phosphatase inhibitors, tumbled overnight at 4°C, and centrifuged. The supernatant contained the NaCl-soluble collagen (non-crosslinked collagen), while the pellet contained the NaCl-insoluble collagen (mature cross-linked fibrillar collagen). For the subsequent steps, each collagen fraction was processed separately. Collagen fractions underwent complete acid hydrolysis with 6N HCl for 18 hours at 120°C, then neutralized to pH 7 with 12N

NaOH. For 50 μ L of sample fraction, 25 μ L of 1.4% chloramine T solution (dissolved in 50% n-propanol, and 1M citrate buffer, pH 6.5) was added at 1:5 ratio for hydroxyproline oxidation, and incubated for 20 minutes at room temperature. Ehrlich's reagent (60% perchloric acid, 15mL n-propanol, and 3.75g *p*-dimethyl-amino-benzaldehyde) was added to neutralize the chloroamine T (20 minutes, 60°C). Absorbance was measured at 558 nm. Soluble and insoluble collagen fraction contents are reported as micrograms of hydroxyproline per milligram LV dry weight (μ g/mg tissue). Total collagen content was calculated as the sum of the soluble collagen and the insoluble collagen.

2.7 Second harmonic generation

Whole frozen mouse heart tissues were thawed at room temperature and immobilized on a flat surface inside a small dish. These unstained unfixed heart tissues were washed several times with the phosphate buffered saline (PBS) solution and finally immersed in the same PBS solution. Second harmonic generation (SHG) and multiphoton excitation fluorescence (MPEF) microscopy methods were used to show the structural remodeling of the collagen matrix in these ex-vivo mouse heart tissues. The nonlinear optical imaging methods are as described previously.¹⁷⁴ Specifically, a femtosecond IR laser source can induce harmonic generation signals from fibrillar collagens, enabling direct visualization of fibrillar collagens without the use of exogenous probes, histological sectioning or staining. The laser used for SHG as well as the endogenous fluorescence emissions was a mode-locked femto-second Spectra-Physics InSight DS femtosecond single-box

laser system with automated dispersion compensation tunable between 680-1300 nm (Spectra-Physics, Mountain View, CA). The laser output was attenuated using AOTF and the average power was consistently maintained below the damage threshold of the samples. The power attenuated laser was directed to a Nikon scan head coupled with Nikon upright microscope system (Nikon Instruments, New York). The laser beam tuned to 880 nm was then focused on the specimen through a high numerical aperture, low magnification, long working distance, dipping objective, CFI75 Apo Water 25X/1.1 LWD 2.0mm WD specifically designed for deep tissue imaging and other *ex vivo* / *in vivo*/ *in vitro* imaging. Upon entering the microscope, the laser beam was directed to the scanning mirrors and subsequently focused on the specimens. The backscattered emission from the sample was collected through the same objective lens. Nikon Element Software was used for the image acquisition. In the reflection mode, non-descanned high-sensitivity GaAsP detectors were used for very efficient SHG and endogenous fluorescence signals. A 750 nm Dichroic was used to prevent the scattered IR laser radiation from reaching the detector and a 460 nm long pass dichroic beam splitter (460 XLRU, Chroma Technology, USA) was used to separate SHG signal from the other endogenous fluorescence signals.

For 3D image data set acquisition, the multiphoton excitation beam tuned to 880 nm was first focused at the maximum signal intensity focal position within the tissue sample and the appropriate detector levels (both the gain and offset levels) were then selected to obtain the pixel intensities within range of 0-4095 (12-bit images)

using a color gradient function. Later on, the beginning and end of the 3D stack (i.e. the top and the bottom optical sections) were set based on the signal level degradation. The 3D stack images with optical section thickness (z-axis) of approximately 1.0 μm were captured from tissue volumes. For each tissue volume reported here, z-section images were compiled and finally the 3D image restoration was performed using VOLOCITY (Perkin Elmar, UK). We calculated the voxel volume of the 3D image data set occupied fibrillar collagens using the following procedure. The volume estimation was performed on the 3D SHG image data sets recorded from at least 5 different areas. The depth of the tissue subjected to the analysis $\sim 200 \mu\text{m}$ thickness. We applied a noise removal filter whose kernel size of 3X3 to remove noise, and the lower threshold level in the histogram was set to exclude all possible background voxel values. Sum of all the voxels above this threshold level is determined to be total fibrillar collagens volume. We then systematically compared 3D image volume of tissues generated using similar imaging conditions. Student t-tests were used to evaluate statistical significance with a $p < 0.05$ considered to be statistically significant.

2.8 Adult cardiac fibroblast isolation and culture

CFBs (cardiac fibroblasts) were isolated from adult WT and *Adam15*^{-/-} mice. 11-13 week old mice were injected with 0.05 mL of 1000 USP/mL heparin for 15 minutes prior to being anesthetized with 2% isoflurane. The heart was excised

and perfused at a constant flow (4 mL/min) with perfusion buffer followed by digestion solution containing collagenase type 2 (Worthington). The LV was separated and dissociated into small pieces using forceps and a transfer pipette in stopping buffer (perfusion buffer + 10% fetal bovine serum [FBS]).

Cardiomyocytes and cFBs were separated by differential centrifugation. The cFB fragment was centrifuged (1500 rpm) and plated in culture dishes coated with 1% gelatin (Sigma). cFBs were cultured in DMEM + 10% FBS (Gibco) in a humidified incubator (37C, 5% CO₂), and were used in the described experiments at passage 2. Prior to experiments, cells were cultured under serum-deprived conditions for 24 hours. The cFBs were randomized into 2 groups and treated for 24 hours: (1) Control, cells were changed to fresh Eagle's DMEM and incubated under normoxic conditions (21% Oxygen); (2) Nutrient deprivation, cells were incubated in Kreb's modified buffer (120.4mM NaCl, 14.7mM KCl, 0.6mM KH₂PO₄, 0.6mM Na₂HPO₄, 1.2mM MgSO₄- 7H₂O, 10mM Na-HEPES, 4.6mM NaHCO₃ and 1mM CaCl₂) and incubated under normoxic conditions (21% oxygen) [5]; (3) Hypoxic, cells were incubated in fresh Eagle's DMEM and incubated under hypoxic conditions (1% Oxygen); (4) Ischemia, cells were incubated in Kreb's modified buffer (120.4mM NaCl, 14.7mM KCl, 0.6mM KH₂PO₄, 0.6mM Na₂HPO₄, 1.2mM MgSO₄- 7H₂O, 10mM Na-HEPES, 4.6mM NaHCO₃ and 1mM CaCl₂) and incubated under hypoxic conditions (1% oxygen). At the end of the protocol cFBs were fixed for immunostaining with 4% paraformaldehyde, or harvested for protein or mRNA analyses as before.¹⁷⁵

2.9 Statistical Analysis

All statistical analysis was performed using the IBM SPSS software. All data were tested for normal distribution by the Shapiro-Wilks Normality Test. The comparison among groups was performed using two-way ANOVA followed by the Bonferroni post-hoc test. Unpaired student's *t*-test was used for comparison between two groups. Averaged values are presented as Mean \pm SEM. Statistical significance was recognized at $p < 0.05$.

Chapter 3

Results

3.1 Loss of ADAM15 impairs recovery from myocardial infarction

We investigated the role of ADAM15 in post-MI remodeling in response to a permanent ligation of the LAD. Protein levels of ADAM15 were decreased in the infarcted region of WT mice following MI compared to the WT sham group (Figure 3Ai). The peri-infarcted and non-infarcted region of the WT hearts had similar protein levels of ADAM15 as the WT sham group. In the ischemic heart of humans, ADAM15 was decreased when compared to the non-failing control (Figure 3Aii). After 1 week of ligation *Adam15*-deficient mice had 28 cumulative (out of 49 total mice) LV rupture deaths compared to 2 LV rupture deaths in WT mice (out of 21 total mice) (Figure 3B). Trichrome staining highlights the dilation and subsequent infarct expansion in the WT and *Adam15*^{-/-} mouse hearts at 3 days and 1-week post-MI (Figure 3C). Ultrasound analyses at 3d post-MI indicated reduced LV function in *Adam15*^{-/-} mice. *Adam15*^{-/-} mice show higher WSMI (2.2 vs 1.8), and less EF (24% vs. 30%) compared to WT; but this difference goes away at 1 week, perhaps because the susceptible mice die of rupture between days 3 and 7 post-MI (Table 3.1). The left atrial size was increased in both genotypes following MI and the *Adam15*^{-/-} 1-week post-MI showed the largest increase. Both systolic and diastolic volume were increased post-MI for both genotypes, which illustrates the extent of LV dilation. At 3 days post-MI, *Adam15*^{-/-} mice had a reduced cardiac output compared to both *Adam15*^{-/-} sham and the corresponding WT group. This rebounded at 1-week post-MI as both *Adam15*^{-/-} and WT mice had similar cardiac outputs compared to their respective shams. Both 3 days and 1-week post-MI mice experienced a

drastic decrease in the fractional area change. The heart wall parameters (IVS, LVID, LVPW) highlight the drastic thinning of the heart wall and expansion of the LV chamber that occurs post-MI for both genotypic mice. The isovolumic relaxation time and isovolumic contraction time are both impaired post-MI with *Adam15*^{-/-} 3 days post-MI having a more severe impairment than the WT counterpart. The E-wave and A-wave are decreased in both *Adam15*^{-/-} and WT mice following MI, which indicates impaired LV filling and diastolic dysfunction. The global longitudinal strain (GLS) is impaired post-MI as the less negative a number the worse the impairment.

Although GLS did not show a difference between genotypes post-MI, it is possible to analyze specific segments of the heart for their own longitudinal strain. These segments are the anterior base, anterior mid, anterior apex, posterior base, posterior mid, and posterior apex. As the infarct expands in post-MI hearts it begins to occupy more of the previously mentioned segments, limiting their movement. As shown in Figure 4A, the strain analysis indicates an increasing ventricular dyssynchrony with time post-MI. It also highlights how different segments are affected with infarct expansion. Figure 4B is the quantification of the peak longitudinal strain present during a heartbeat for each segment. Following MI, both WT and *Adam15*^{-/-} mice have impaired strain in the anterior and posterior apex, the anterior and posterior mid, and the anterior base. The key finding was that the endocardial side of the posterior base in the *Adam15*^{-/-} mice post-MI was drastically worse than the WT mice at both 3 days

and 1-week MI. This could be due to an increased infarct expansion into the region.

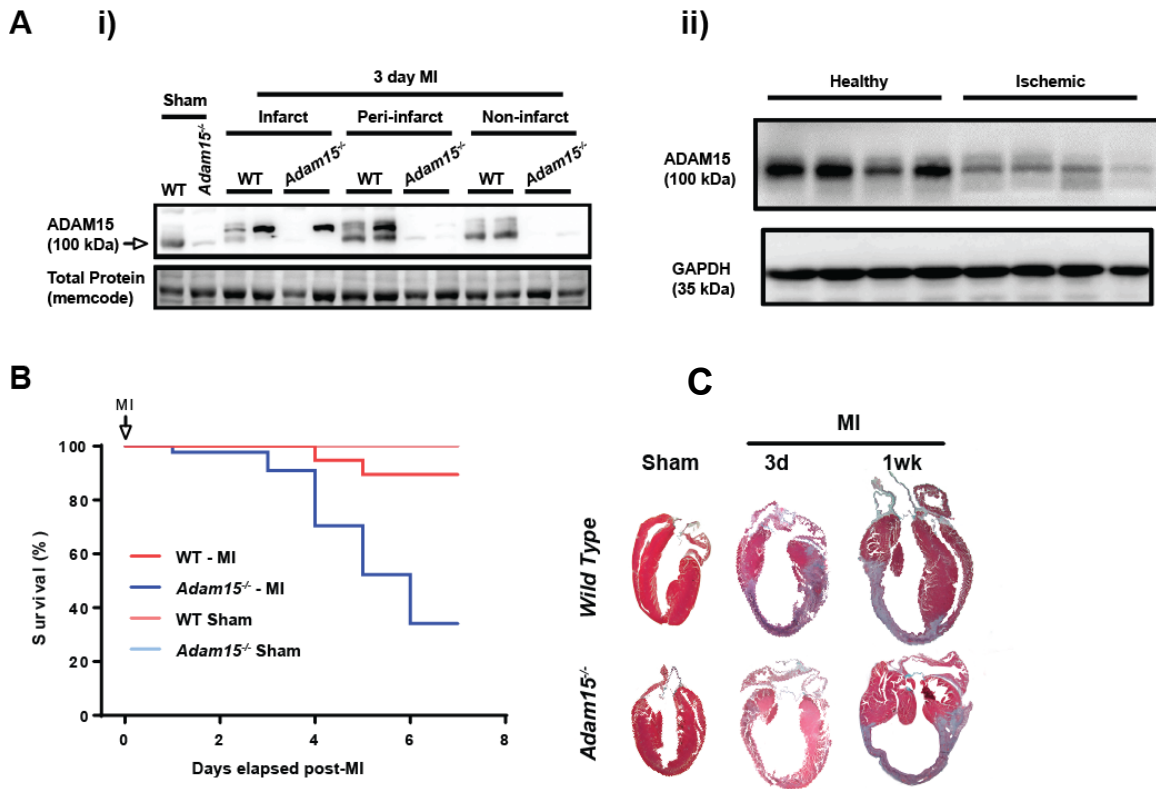


Figure 3. Absence of *Adam15* leads to left ventricular rupture. (Ai)

Representative immunoblot analysis for ADAM15 in the heart from WT and

Adam15^{-/-} mice following sham or MI surgery. (Aii) Representative immunoblot

analysis for ADAM15 from human heart samples. (B) Kaplan-Meier survival

curve showing the percentage of survival after surgery for each genotype. (C)

Representative trichrome staining of whole hearts from WT and *Adam15*^{-/-} mice

at specified time-points

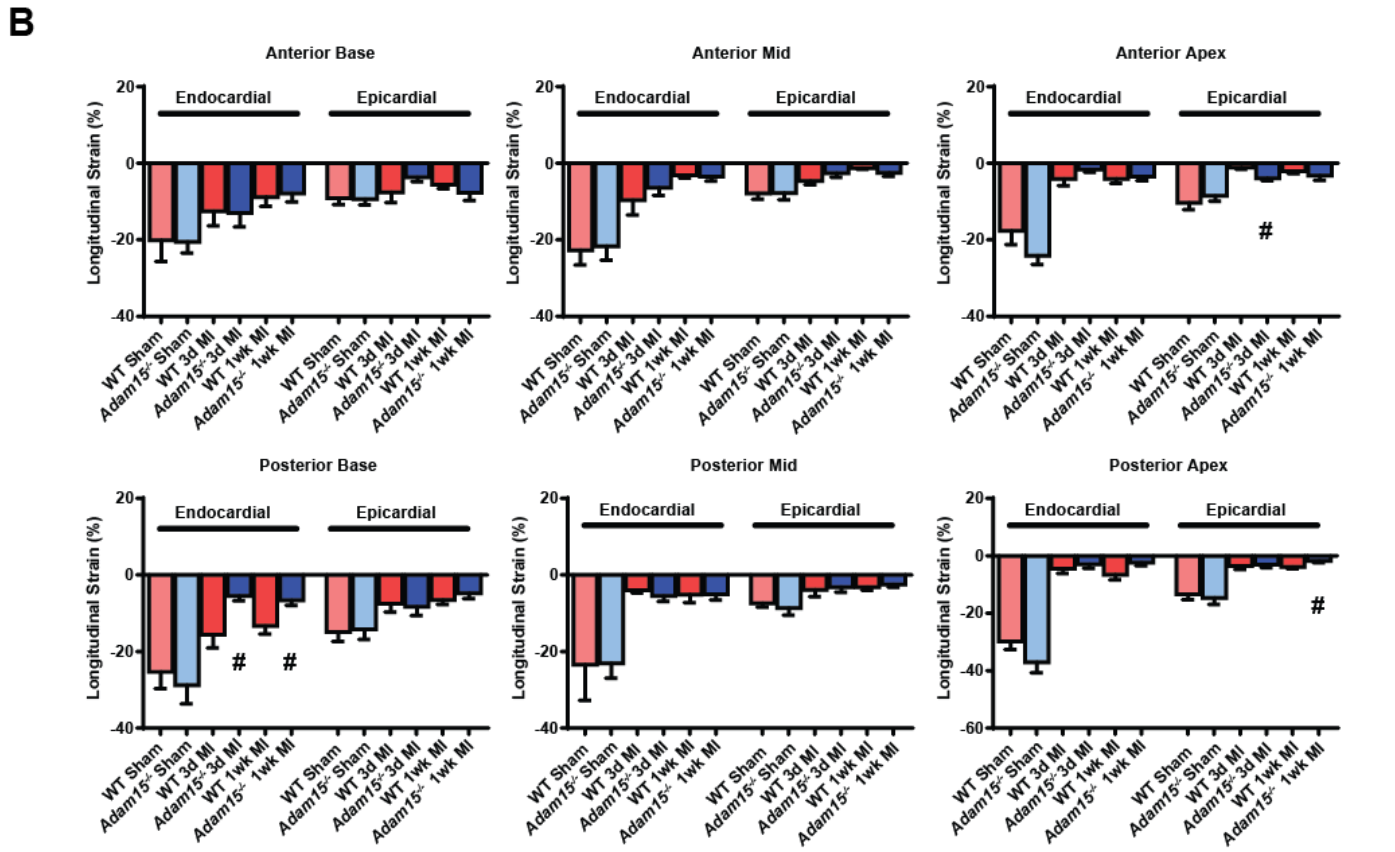
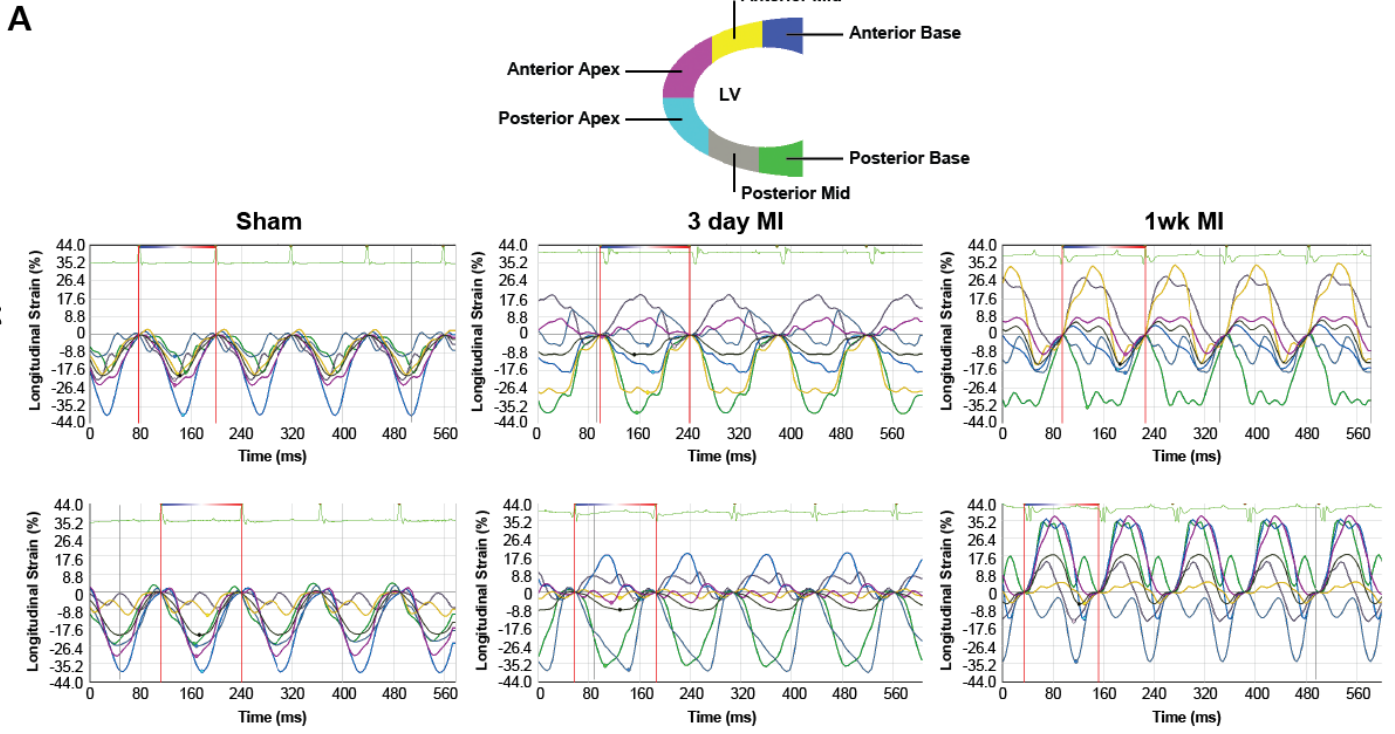


Figure 4. Loss of *Adam15* impairs contraction of the posterior base at 3 days and 1-week post-MI compared to sham groups. (B) Strain quantification of different areas of strain analysis of the LV. Averaged values represent Mean \pm SEM. Sample size n=7-13 hearts/genotype/group. #*p* < 0.05 vs corresponding WT group.

Parameters	Sham		3-day MI		1-week MI	
	WT	ADAM15KO	WT	ADAM15KO	WT	ADAM15KO
<i>n</i>	10	14	9	8	12	12
LV Systolic Volume, μ L	27.7 \pm 2.8	25.8 \pm 1.5	64.9 \pm 5.7*	69.8 \pm 5.2*	106.0 \pm 9.4*	110.6 \pm 10.7*
LV Diastolic Volume, μ L	65.7 \pm 4.3	61.7 \pm 2.9	91.7 \pm 5.7*	91.2 \pm 6.5*	139.1 \pm 9.2*	142.6 \pm 11.3*
LV Ejection Fraction, %	58.3 \pm 2.4	58.0 \pm 1.8	30.1 \pm 2.1*	21.4 \pm 1.6#*	24.9 \pm 2.1*	23.3 \pm 1.8*
CO, mL/min	18.0 \pm 1.4	16.7 \pm 1.2	14.0 \pm 0.7*	10.2 \pm 0.8#*	17.4 \pm 1.2	16.1 \pm 1.5
FAC, %	47.7 \pm 3.5	50.2 \pm 2.5	15.7 \pm 3.2*	11.8 \pm 2.1*	7.8 \pm 1.8*	10.9 \pm 2.7*
Heart Rate, beats/min	467 \pm 16	466 \pm 9	522 \pm 21	466 \pm 8#	500 \pm 13	482 \pm 18
WMSI	1.00 \pm 0.00	1.00 \pm 0.00	1.83 \pm 0.04*	2.10 \pm 0.05#*	2.05 \pm 0.08*	2.11 \pm 0.06*
GLS, %	-21.6 \pm 1.00	-24.2 \pm 2.22	-6.57 \pm 1.12*	-3.91 \pm 1.01*	-4.06 \pm 1.12*	-3.01 \pm 0.73*
Left Atrial Size, mm	1.98 \pm 0.08	1.89 \pm 0.1	2.64 \pm 0.11*	2.75 \pm 0.18*	2.16 \pm 0.12*	2.64 \pm 0.12#*

IVSd, mm	0.83 ± 0.13	0.69 ± 0.03	0.66 ± 0.05*	0.64 ± 0.11	0.56 ± 0.04*	0.76 ± 0.09
IVSs, mm	1.00 ± 0.03	1.05 ± 0.06	0.80 ± 0.07*	0.71 ± 0.12*	0.63 ± 0.05*	0.94 ± 0.13
LVIDd, mm	3.78 ± 0.07	3.90 ± 0.10	4.61 ± 0.16*	4.66 ± 0.12*	5.79 ± 0.18*	5.26 ± 0.29*
LVIDs, mm	2.73 ± 0.07	2.69 ± 0.07	4.01 ± 0.23*	4.36 ± 0.12*	5.45 ± 0.19*	4.73 ± 0.38*
LVPWd, mm	0.74 ± 0.05	0.80 ± 0.03	0.80 ± 0.08	0.59 ± 0.05#*	0.75 ± 0.06	0.84 ± 0.09
LVPWs, mm	1.06 ± 0.06	1.15 ± 0.03	0.94 ± 0.08	0.65 ± 0.06#*	0.86 ± 0.07*	0.98 ± 0.12
E-wave, mm/s	481.1 ± 44.2	457.6 ± 20.2	359.6 ± 30.5*	269.6 ± 17.3*	342.3 ± 36.5*	317.0 ± 42.2*
A-wave, mm/s	330.1 ± 38.2	305.4 ± 22.9	203.2 ± 55.7	155.9 ± 14.1*	180.2 ± 15.4*	125.4 ± 41.6*
DT, ms	17.4 ± 1.1	15.3 ± 1.5	8.5 ± 1.7*	10.8 ± 1.6	11.5 ± 1.8*	6.7 ± 1.3#
IVRT, ms	14.0 ± 0.9	13.2 ± 0.50	18.1 ± 0.9*	22.0 ± 0.5#*	22.4 ± 1.7*	22.5 ± 1.6*
IVCT, ms	12.6 ± 0.9	12.5 ± 0.7	19.6 ± 1.0*	20.5 ± 1.2*	19.7 ± 1.4*	23.8 ± 1.7
E/A	1.5 ± 0.1	1.6 ± 0.1	2.5 ± 1.4	1.6 ± 0.3	2.3 ± 0.2*	2.1 ± 0.6
E', mm/s	19.7 ± 2.3	19.9 ± 1.4	14.4 ± 1.6	9.5 ± 1.7*	14.1 ± 1.6	12.3 ± 2.0
A', mm/s	15.0 ± 0.1	16.0 ± 1.0	11.6 ± 1.2*	8.3 ± 1.3*	14.3 ± 1.2	12.5 ± 2.2
E'/A'	1.4 ± 0.1	1.2 ± 0.05	1.3 ± 0.1	1.3 ± 0.3	1.0 ± 0.1*	1.0 ± 0.07*

A'/E'	0.8 ± 0.06	0.8 ± 0.03	0.8 ± 0.06	1.0 ± 0.2	1.1 ± 0.1	1.06 ± 0.11
E/E'	26.6 ± 2.8	22.0 ± 1.3	26.9 ± 3.1	34.6 ± 6.1	29.7 ± 3.3	29.3 ± 3.7

Table 3.1 Echocardiographic assessment of heart function in WT and *Adam15*^{-/-} mice and corresponding shams at 3 days and 1-week post-MI.

LV=Left ventricle; CO=Cardiac output; FAC=Fractional area change; WMSI=Wall motion score index; GLS=Global longitudinal strain; IVS=Interventricular septum at the end of systole (IVSs) or diastole (IVSd); LVID=LV internal diameter at the end of systole (LVIDs) or diastole (LVIDd); LVPW=LV posterior wall thickness at the end of systole (LVPWs) or diastole (LVPWd); E-wave=early transmitral peak velocity; A-wave=transmitral inflow velocity due to atrial contraction; DT=deceleration time of E-wave; IVRT=Isovolumic relaxation time; IVCT=Isovolumic contraction time; E'=Early tissue Doppler velocity; A'=Tissue Doppler velocity due to atrial contraction. #*p* < 0.05 between corresponding genotypes. **p* < 0.05 between corresponding sham group.

3.2 Impact of *Adam15*-deficiency in inflammatory response following myocardial infarction

One of the aforementioned characteristics of MI pathogenesis is the infiltration of myocardium by inflammatory cells to clear debris and cells to prepare the myocardium for scar formation. Because ADAM15 has been linked to endothelial permeability and subsequently affects inflammatory infiltration, we investigated if

the severity of inflammation or subpopulations of inflammatory cells in the myocardium post-MI were altered with *Adam15*-deficiency.

Immunohistochemical staining of post-MI hearts using a neutrophil (Ly-6B.2; AbD Serotec) and macrophage (CD68; AbD Serotec) specific antibodies indicated that both the neutrophil and macrophage populations increased in number in the infarcted and non-infarcted region. However, there was no difference between genotypes. (Figure 5A-B). Using Taqman RT-PCR, we quantified the relative expression of pro-inflammatory, antifibrotic M1 (*IL-1 β* , *IL-6*, *Ccl3*, *Mcp-1*, *Cd38*, *Tnfa*) and anti-inflammatory and profibrotic M2 (*Cd168*, *Cd206*, *Egr2*, *Ym1*, *Ccl5*) macrophage phenotypes (Figure 5C-D). *IL-1 β* was increased in both the infarcted and peri-infarcted regions of the heart in both genotypes, but the increase of *IL-1 β* in infarcted region of the WT mice was not mirrored to the same extent in the *Adam15*^{-/-} mice. *IL-6*, *Ccl3*, and *Mcp-1* were increased globally throughout the hearts of both *Adam15*^{-/-} and WT mice following MI with the infarcted region showing the greatest increase. *Ccl3*, like *IL-1 β* , was decreased in the infarct of *Adam15*^{-/-} mice compared to the infarcted region of the WT mice. *Tnfa* was increased in both the infarcted regions *Adam15*^{-/-} and WT mice but there was no genotype specific differences. *Cd168* was increased globally post-MI. *Adam15*^{-/-} mice had less expression of *Cd168* in their peri-infarcted region than the WT mice. *Cd206* was also increased globally following MI, but no region specific increases were identified. *Egr2* expression was similar to *Cd168* in that *Egr2* was globally increased but there was a significant difference between *Adam15*^{-/-} and

WT mice in the peri-infarcted region. *Ym1* showed regional specificity with increases in the infarcted region, and similar increases between the peri-infarcted

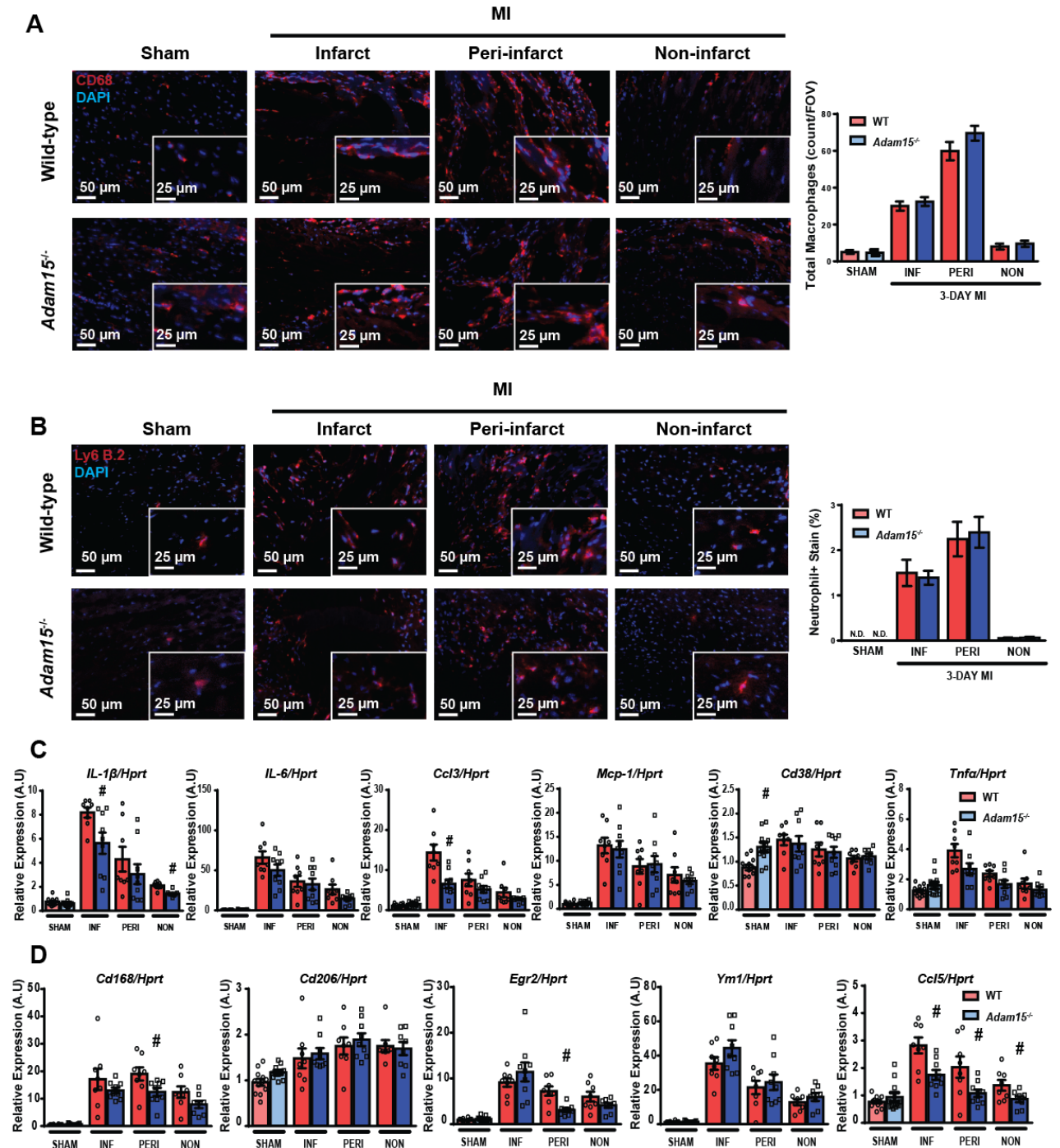


Figure 5. Absence of ADAM15 does not affect the inflammatory response

post-MI. (A) Representative images of macrophage staining with CD68 primary antibody with DAPI nuclear staining. Quantification was done by counting overlaying red and blue stains per field of view. (B) Representative images of neutrophil staining with Ly6 B.2 with DAPI nuclear staining. Quantification was done by computer analysis that counted red pixels that indicated neutrophil positive staining per field of view. (C) mRNA expression of M1 macrophage markers. (D) mRNA expression of M2 macrophage markers. Averaged values represent Mean \pm SEM. N.D. = not detectable. R.E. = relative expression. # $p < 0.05$ vs. corresponding WT group.

3.3 Absence of ADAM15 markedly impairs collagen fiber organization and assembly

Having identified that the inflammatory response could not explain the increased rupture rate of *Adam15*^{-/-} mice, the next logical progression was to identify whether or not fibrosis was the underlying culprit. Fibrosis occurs after the resolution of inflammation. As M1 macrophages phagocytize the remaining neutrophils, they undergo a phenotypic switch to become M2 macrophages.¹⁷⁶ These macrophages release TGF- β and cause cardiac fibroblasts to activate and become cardiac myofibroblasts. These myofibroblasts produce and secrete collagen into the interstitium to fill in the space created by the absence of cardiomyocytes. As we could not identify a specific inflammatory factor that could mediate a difference in LV rupture between genotypes, fibrosis (or lack thereof) could be the mediating factor. Following this process of fibrosis, we decided to

examine the protein and mRNA expression of collagen, collagen cross-linking enzyme lysyl oxidase-1 (LOX-1), the separate fractions of cross-linked versus noncross-linked collagen, the activation of myofibroblasts, and the morphology of the collagen present using second harmonic generation (SHG) of the WT and *Adam15*^{-/-} mice post-MI.

We found that the collagen fibers in the infarct region of *Adam15*^{-/-} mice were more sparse and more disarrayed compared to WT mice, as shown by SHG imaging and quantification (Figure 6A). Using a hydroxyproline assay, we separated the cross-linked (insoluble) and noncross-linked (soluble) collagen fractions. *Adam15*^{-/-} mice had decreased cross-linked collagen and increased noncross-linked collagen (Figure 6B). Total collagen (soluble + insoluble collagen) was decreased in the infarcted region of the *Adam15*^{-/-} hearts, similar to the SHG imaging. LOX-1, a collagen cross-linking enzyme, had reduced expression and protein levels in the *Adam15*^{-/-} mice post-MI compared to the WT mice (Figure 6Ci/ii). This may be the protein responsible for the reduced cross-linking seen in the hydroxyproline assay.¹¹² mRNA expression of *Col1α1* and *Col1α2* were reduced in *Adam15*^{-/-} mice hearts post-MI in the peri-infarcted and non-infarcted regions, whereas *Col3α1* was increased in the non-infarcted region of *Adam15*^{-/-} mice hearts compared to the WT mouse hearts (Figure 6D). This is also a contributing factor to rupture, as with less collagen expression there will be less scar formation and increased rupture susceptibility. *αSMA* expression, a marker of cardiac myofibroblast transformation, was decreased in the hearts of

Adam15^{-/-} mice compared to the WT mice post-MI in the peri-infarcted and non-infarcted regions (Figure 6D). As it was not different between genotypes in the infarcted area, this may suggest that myofibroblast transformation has multiple pathways that are activated without the presence of ADAM15 in a severely damaged area such as the infarct zone. However, these pathways may not activate in less damaged areas, such as the peri- and non-infarcted regions, and the loss of ADAM15 is noticeable on myofibroblast transformation. This difference is also reflected in collagen expression in these hearts, where the increased presence of myofibroblasts in the infarcted area mirrors the increased expression of collagen.

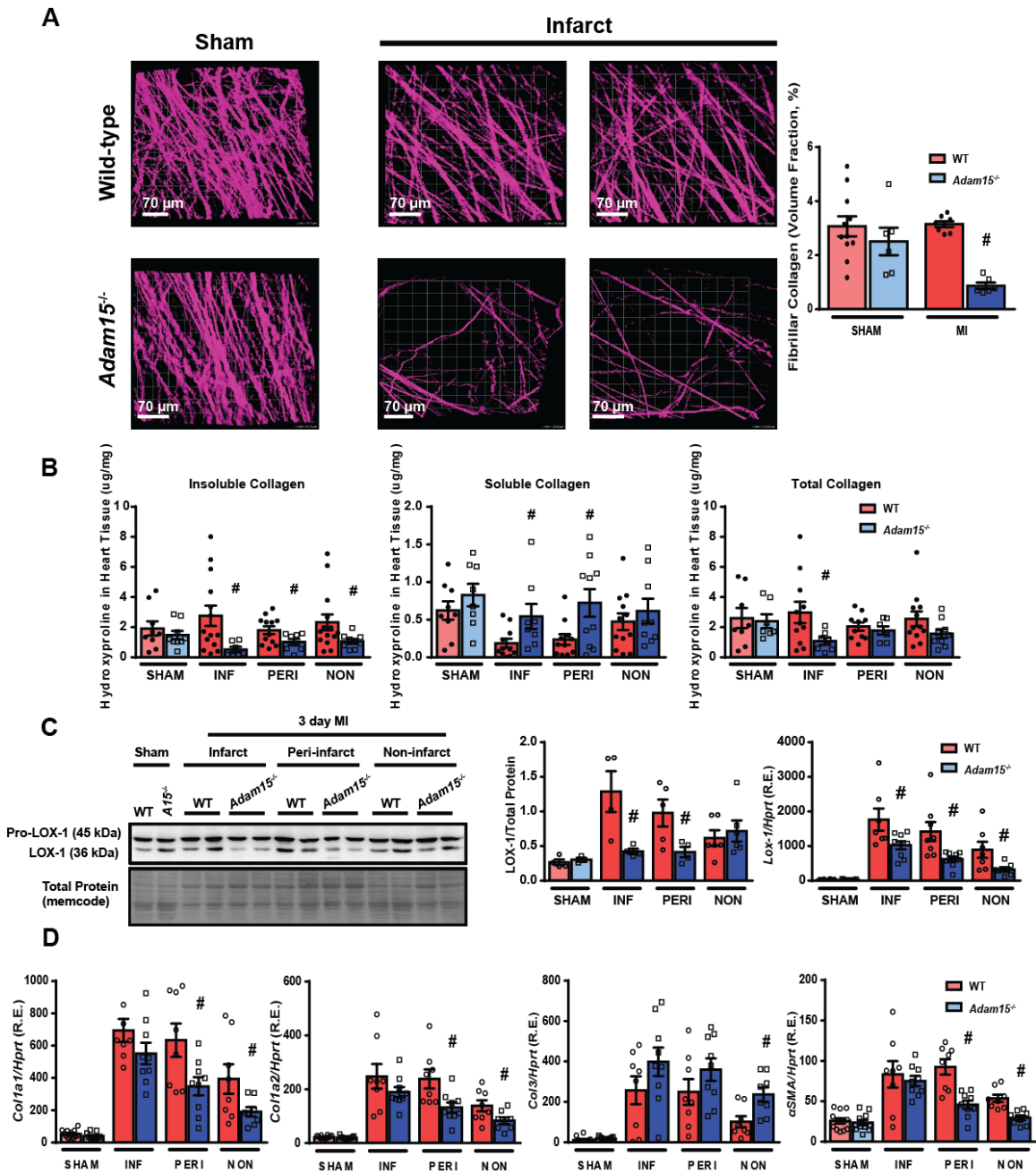


Figure 6. Absence of ADAM15 attenuates fibrotic response to a myocardial infarction. (A) Representative second harmonic generation (SHG) images, and their quantification after sham or MI surgery. (B) Hydroxyproline assay results quantifying the cross-linked (insoluble), noncross-linked (soluble) and total (insoluble + soluble) collagen in the heart post-MI. (C) Representative

immunoblots, quantification and expression of collagen cross-linking enzyme LOX-1. (D) TaqMan mRNA expression of fibrotic markers in the heart after MI in the indicated groups. HPRT=Hypoxanthine-guanine phosphoribosyltransferase. LOX-1=Lysyl oxidase-1 (protein); *Lox-1*=Lysyl oxidase-1 (mRNA). *Col1 α 1*=Collagen type I alpha 1 chain (mRNA); *Col1 α 2*=Collagen type I alpha 2 chain (mRNA); *Col3 α 1*=Collagen type III alpha 1 chain (mRNA); α SMA=alpha smooth muscle actin. Averaged values represent Mean \pm SEM. #*p*<0.05 vs. corresponding WT group.

3.4 Reduced fibronectin content in the *Adam15*-deficient infarcted myocardium

Activation of myofibroblasts is a critical step in fibrosis, and as such we looked for a possible link between ADAM15 and this activation process. Reduced myofibroblast activation leads to reduced collagen production, cross-linking and deposition. As shown previously through α SMA expression, *Adam15*^{-/-} mice hearts post-MI have reduced myofibroblast activation in the peri-infarcted and non-infarcted regions as compared to WT counterparts. Fibronectin (FN) has previously been found to be necessary for myofibroblast activation following an ischemic event in the heart, and that FN is elevated in post-MI hearts.¹⁷⁷ We found that *Adam15*^{-/-} mice post-MI had reduced fibronectin protein levels in the infarcted myocardium *in vivo* (Figure 7Ai) and reduced mRNA expression of *Fn-1* in the infarcted and peri-infarcted regions (Figure 7Aii) compared to the WT mice. Fibronectin protein and expression was elevated in both *Adam15*^{-/-} and WT mice

in the infarct more so than the peri-infarcted regions. Immunostaining was performed, and the reduction in fibronectin in the infarcted regions of the *Adam15*^{-/-} mice hearts was visualized (Figure 7B). The higher magnification insets highlight the disparity between the infarcted regions of the *Adam15*^{-/-} and WT mice, while the sham, peri-infarcted, and non-infarcted regions are less easily distinguished between the genotypes.

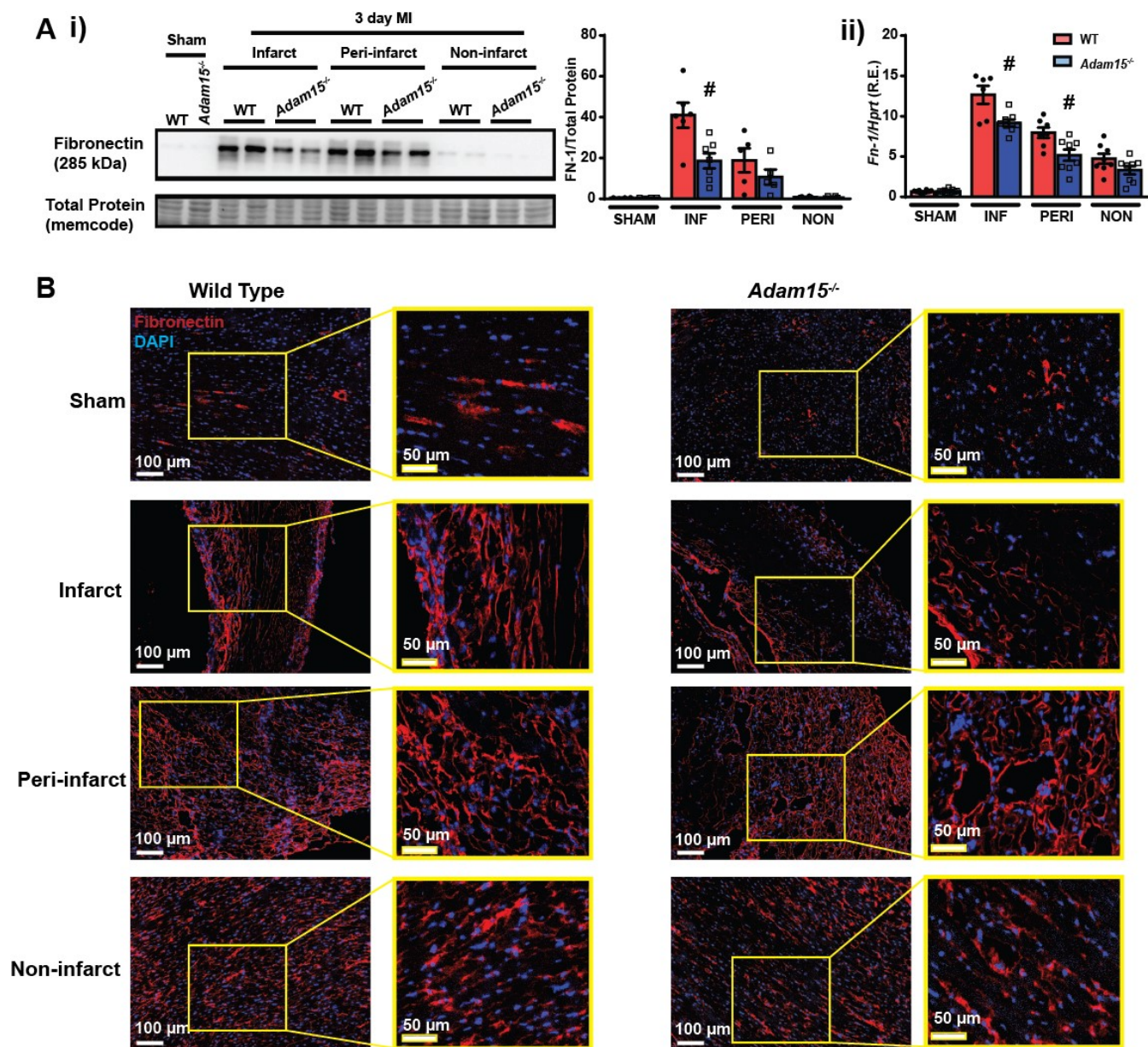


Figure 7. *Adam15*-deficient mice have reduced fibronectin expression and secretion. (Ai) Representative immunoblot and quantification of fibronectin. (Aii) Quantification of fibronectin expression *in vivo*. (B) Representative immunofluorescent staining for fibronectin after sham or MI surgery. Insets show higher magnification image. HPRT=Hypoxanthine-guanine

phosphoribosyltransferase. FN-1=Fibronectin (protein); *Fn-1*=Fibronectin (mRNA). Averaged values represent Mean \pm SEM. # p <0.05 vs. corresponding WT group.

3.5 In adult cardiac fibroblasts lacking ADAM15, activation in response to ischemia is suppressed

To assess the possibility that ADAM15 can influence the activation of myofibroblasts, we isolated cardiac fibroblasts (cFBs) from both *Adam15*^{-/-} and WT hearts to assess the possible role of ADAM15. Using an *in vitro* ischemia model (hypoxic environment with a lack of nutrients, e.g. glucose, amino acids, etc.), our goal was to eliminate other external influences and have the cells subjected to experimentation generate their own microenvironment within the cell culture dishes in response to the experimental stimuli. We found that WT cFBs showed decreased ADAM15 protein levels in the nutrient deprivation and ischemia groups compared to the normoxia group (Figure 8A). We surmised that ADAM15 plays a role in myofibroblast activation, and that it could be through fibronectin. Fibronectin protein and expression is decreased in both *Adam15*^{-/-} and WT cFBs in the ischemia group, with *Adam15*^{-/-} cFBs having less fibronectin protein and mRNA than WT cFBs (Figure 8B). *Adam15*^{-/-} cFBs did not undergo transformation into myofibroblasts whereas the WT cFBs showed marked increase in α SMA in response to ischemia (Figure 8C). Normoxia and nutrient deprivation did not affect α SMA staining in either genotype, but both hypoxia and ischemia groups increased α SMA staining in the WT but not *Adam15*^{-/-} cFBs. This highlights the activation of fibroblasts in response to the *in vivo* related

experimental ischemic group. LOX-1 was decreased uniformly in the ischemic group of both genotypes as compared to the normoxia treated cFBs (Figure 8D).

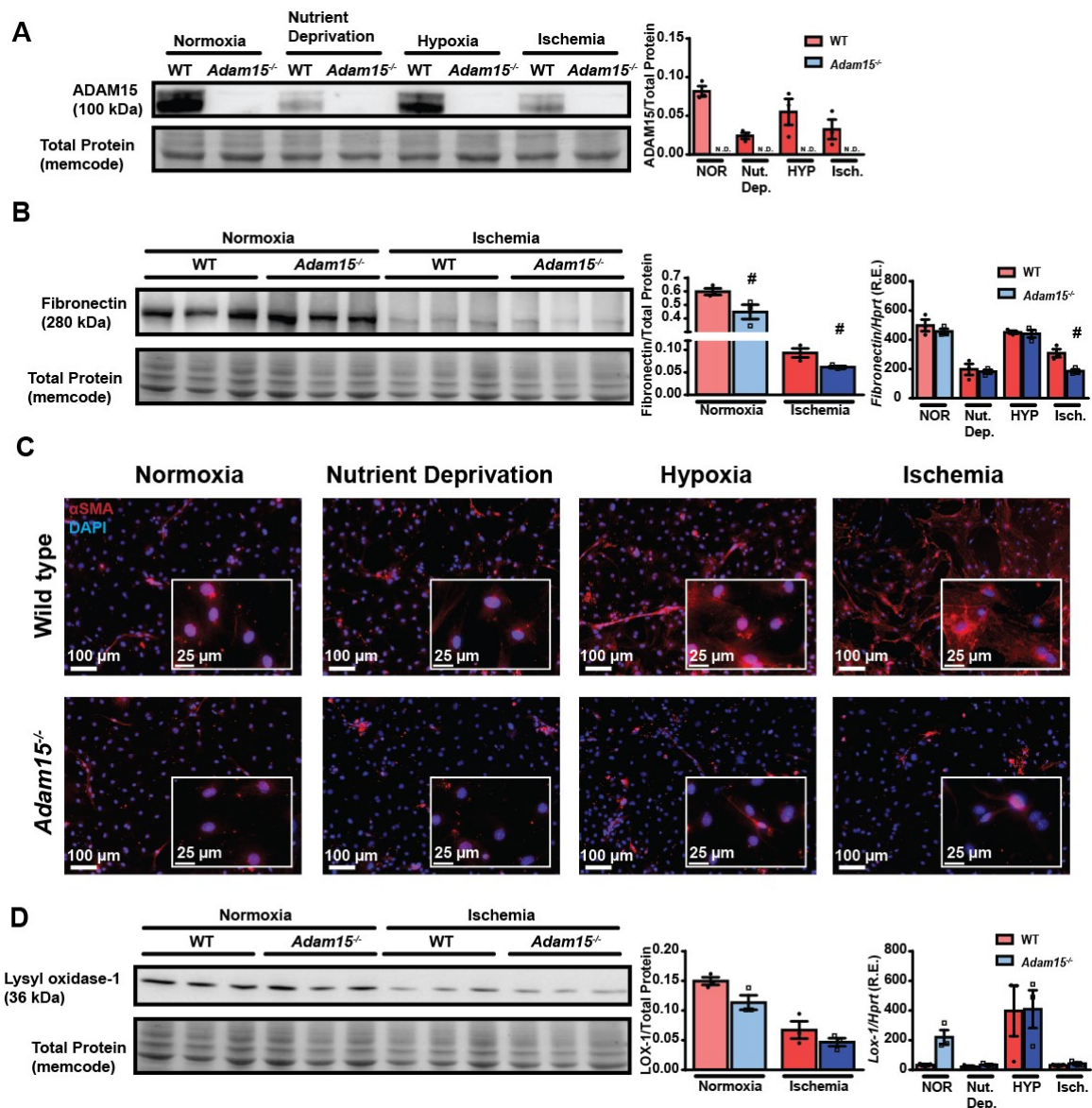


Figure 8. Presence of ADAM15 promotes activation of fibroblasts. (A)

Representative immunoblot, and quantification of ADAM15 in cardiac fibroblasts in their respective experimental conditions *in vitro*. (B) Representative immunoblot, quantification, and expression of fibronectin in cardiac fibroblasts in their respective experimental conditions *in vitro*. (C) Representative immunofluorescent staining of α -smooth muscle actin (α SMA; red), a marker for myofibroblast transformation, of cardiac fibroblasts in their respective experimental conditions *in vitro*. Insets show higher magnification image. (D)

Representative immunoblot, quantification, and expression of lysyl oxidase-1 in cardiac fibroblasts in their respective experimental conditions *in vitro*. Averaged values represent Mean \pm SEM. # $p < 0.05$ vs. corresponding WT group.

3.6 ADAM15 initiates activation of PAK1 and induces expression of Fibronectin and Lox1 *in vivo* and *in vitro*

We identified p21-activated kinase-1 (PAK-1) as a possible protein to link fibronectin to ADAM15. PAK-1 is a transcription factor that promotes fibronectin transcription.¹⁷⁸ As such, we began looking at the protein expression of PAK-1. We found that PAK-1 is decreased, compared to WT mice, in the infarcted, peri-infarcted and non-infarcted regions of *Adam15*^{-/-} mice post-MI (Figure 9A). It is also decreased *in vitro* in the ischemic group of isolated cardiac fibroblasts from *Adam15*^{-/-} mice (Figure 9B). This led us to determine whether ADAM15 interacts with PAK-1. Using a proximity ligation assay (PLA) on histological samples, we found that ADAM15 physically interacts with PAK-1, with more interactions occurring in the infarcted and peri-infarcted region of the WT mice (Figure 9C). This highlights that ADAM15 is required for PAK1 to induce fibronectin expression and cause myofibroblast transformation.

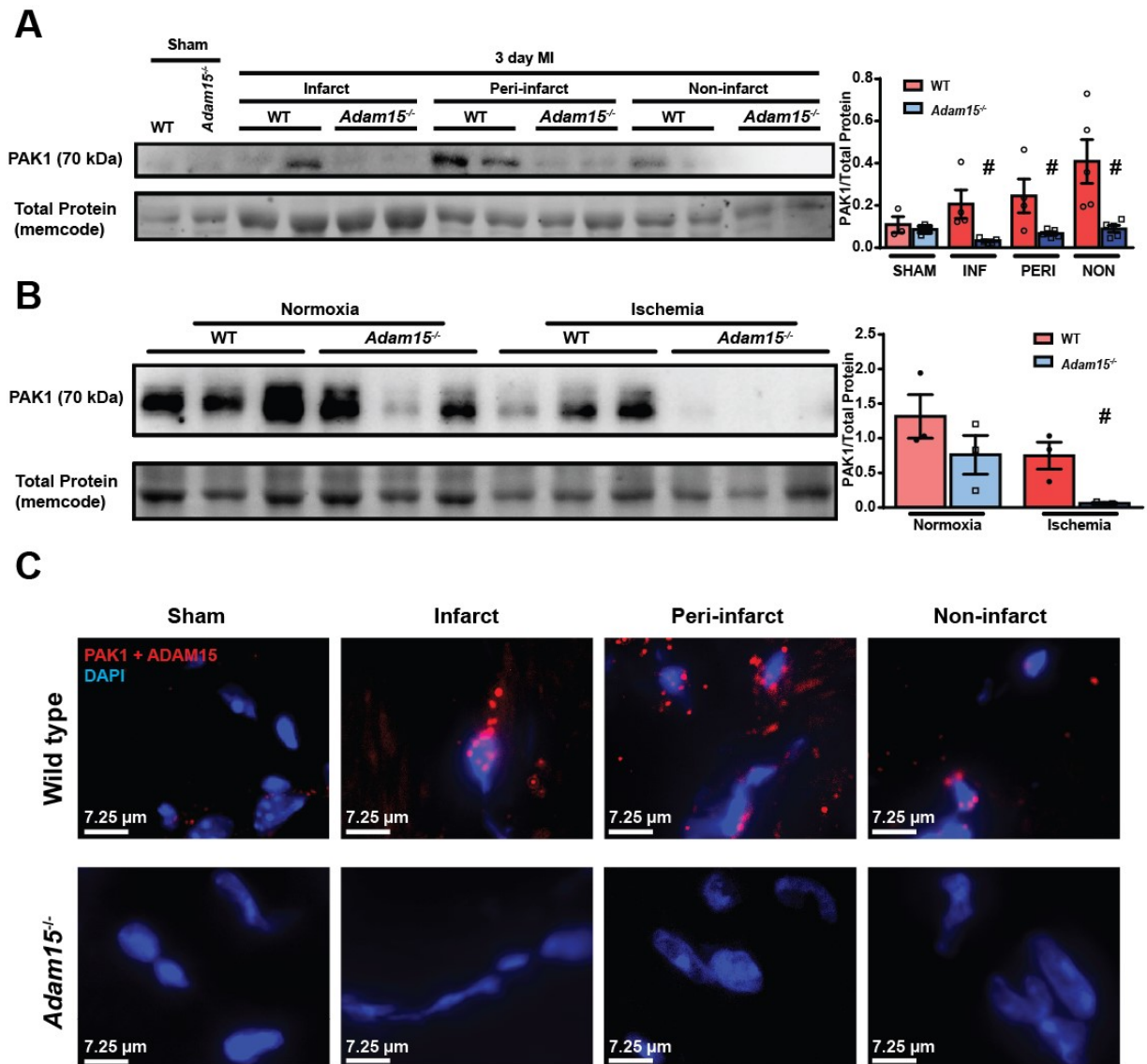


Figure 9. ADAM15 interacts with PAK1. (A) Representative immunoblot and quantification of PAK1 in sham and MI hearts. (B) Representative immunoblot and quantification of PAK1 protein levels in primary cardiac fibroblast culture. (C) Representative immunostaining of proximity ligation assay images for the interaction of PAK1 and ADAM15 in heart samples. *In vitro* ischemia was achieved by nutrient and oxygen depletion. Averaged values represent Mean \pm SEM. # $p < 0.05$ vs. corresponding WT group.

Chapter 4

Discussion

4.1 Discussion

Myocardial remodeling after MI is a multifactorial process involving numerous cellular and molecular events. As blood flow is stopped to the myocardium, cardiomyocytes begin to undergo necrosis triggering an influx of inflammatory cells. Neutrophils and macrophages clear the wound of debris and dead/damaged cardiomyocytes. The inflammatory response is resolved when neutrophils have undergone apoptosis, and this process facilitates scar formation to replace the dead cardiomyocytes. Cardiac fibroblasts transform into myofibroblasts and begin to deposit collagen to form the scar. Patient treatment post-MI has focused on preventing further ischemic events and restoring blood flow to the previously ischemic area. Many studies have focused on reducing the long-term impact of the ischemic event on the surrounding, unaffected myocardium as reactive fibrosis can cause damage to this myocardium.¹⁷⁹⁻¹⁸²

ADAM15 has been involved in the role of angiogenesis and endothelial permeability and this was the initial reason to investigate the role of ADAM15 in post-MI remodeling. ADAM15 promotes endothelial permeability and a deletion of ADAM15 could limit inflammatory cell infiltration into the infarcted area and the collateral damage inflammation induces.¹⁶³

4.2 The increased rate of LV rupture in *Adam15*^{-/-} mice post-MI is not the result of heightened inflammatory response

Contrary to our initial hypothesis, *Adam15* deletion is not beneficial in a permanent ligation model of MI. *Adam15*^{-/-} mice had a marked increase in the

rate of LV rupture compared to the WT mice, and *Adam15*^{-/-} mice had reduced LV functionality compared to their WT counterpart at 3 days post-MI as assessed by ejection fraction. The rupture rate of the *Adam15*^{-/-} mice was not associated with an increase in the inflammatory response which has previously been associated with LV rupture.¹⁸³ An increased neutrophil population has previously been associated with LV rupture in humans.¹⁸⁴ Selective depletion of M2 macrophages post-MI resulted in a nine-fold increase in cardiac rupture.¹⁸⁵ Unmitigated IL-1 signaling following MI in a mouse model resulted in poor cardiac remodeling.¹⁸⁶ High serum levels of IL-6 have been found in patients with myocardial infarction and correlate with infarct size.^{42, 187} IL-6 upregulation and increased activation of its common receptor, glycoprotein-130, promotes an increased inflammatory response and LV rupture in mice.¹⁸⁸ All of these markers of inflammation were not affected by the deletion of *Adam15*. It is also important to note that although ADAM15 has been previously linked to endothelial permeability, we did not observe a decrease in inflammatory cell infiltration in the *Adam15*^{-/-} mice.¹⁶⁸ This could be due to a pro-inflammatory state, in the case of chronic LAD ligation, as a result of constant DAMP signaling from damaged cells outweighing any possible benefit of ADAM15 deletion.¹⁸⁹ It could also be due to other mechanisms affecting endothelial permeability, such as intracellular adhesion molecule (ICAM)-1 that facilitates cell adhesion and leukocyte infiltration, that contribute to leukocyte infiltration more than a deletion of *Adam15* attenuates it. ICAM-1 is an adhesion molecule that is upregulated by pro-

inflammatory cytokines.¹⁹⁰ It promotes adhesion of leukocytes to endothelial cells and endothelial permeability.¹⁹¹

In summary, through analyzing the expression of various inflammatory markers and cells we established that the rupture rate seen in *Adam15*^{-/-} mice was not attributable to inflammation.

4.3. ADAM15 plays a key role in myocardial fibrosis in response to a MI

ADAM15 has yet to be identified as a regulator of a fibrotic response, and this is the first report on its role in myocardial fibrosis. At 3 days post-MI in mice, the resolution of inflammation occurs and the reparative phase begins in which fibrotic depositions form a scar in the infarcted region. It was at this transitional period that *Adam15*^{-/-} mice began to show increased rates of LV rupture, which has also been identified by other studies.^{192, 193} We found that loss of ADAM15 impacted the ability of cardiac fibroblasts to transform into myofibroblasts. This attenuated the required fibrotic response to replace the damaged cardiomyocytes, and left the damaged myocardium susceptible to rupture. *Adam15*^{-/-} mice with the reduced presence of myofibroblasts, produced less collagen, and had less cross-linked collagen, via attenuated production of the cross-linking enzyme LOX-1. The results in this thesis have highlighted the necessity of a fibrotic response in MI, but other studies have shown the deleterious affect excessive fibrosis can have. LOX-1 expression is increased in the post-MI infarcted area.¹¹² Type I collagen, secreted by myofibroblasts,

confers tensile strength to the infarct if multiple fibers are cross-linked via LOX-1.¹⁹⁴ Increased collagen cross-linking in the infarct region has been associated with adverse LV remodeling in the non-infarcted region as well.¹¹⁶ Inhibition of LOX-1 has been associated with improved LV function and reduced infarct expansion post-MI in a murine model.¹¹² While excessive collagen cross-linking is detrimental to LV remodeling post-MI, it is also required to prevent rupture as shown in the results section.

The reduced fibronectin observed in the *Adam15*^{-/-} mice post-MI serves two functions in this regard. First, fibronectin interacts with LOX-1 to facilitate its activation and to serve its purpose in cross-linking collagen strands prior to deposition.¹¹³ Secondly, a reduction in fibronectin impacts the transformation of cardiac fibroblasts into myofibroblasts.¹⁸⁰ Fibronectin is upregulated in the infarct of human MI patients and is produced by fibroblasts and endothelial cells.^{177, 195} This multicellular expression of fibronectin explains why the *in vitro* data showed a decrease in the protein levels of fibronectin in response to ischemia yet an increase in fibronectin *in vivo* post-MI as fibroblasts are not the only cell to produce fibronectin in response to an infarct. Fibronectin expression precedes collagen expression in an ischemic area, further highlighting the fact the myofibroblast transformation is not required for initial fibronectin deposition.^{196, 197}

ADAM15 regulates fibronectin expression by interacting with PAK1, likely through its cytosolic domain (Figure 10). Once activated, PAK1 attaches to the fibronectin

promotor region and increases fibronectin transcription.¹⁷⁸ Without this interaction, PAK1-mediated fibronectin transcription is attenuated and the resulting transformation of cardiac fibroblasts does not happen as shown in the results. This impairs scar formation and leads to LV rupture. Our study shows a physical interaction between ADAM15 and PAK1, however it may not be as simple as a 1-to-1 interaction. Both the ADAM15 cytoplasmic tail and PAK1 have SH3 binding domains.^{198, 199} This may mean that ADAM15 and PAK1 bind a similar protein to facilitate the ADAM15/PAK1 interaction. Possible proteins that could mediate the interaction include Lck, Fyn, Abl, and Src.²⁰⁰⁻²⁰³

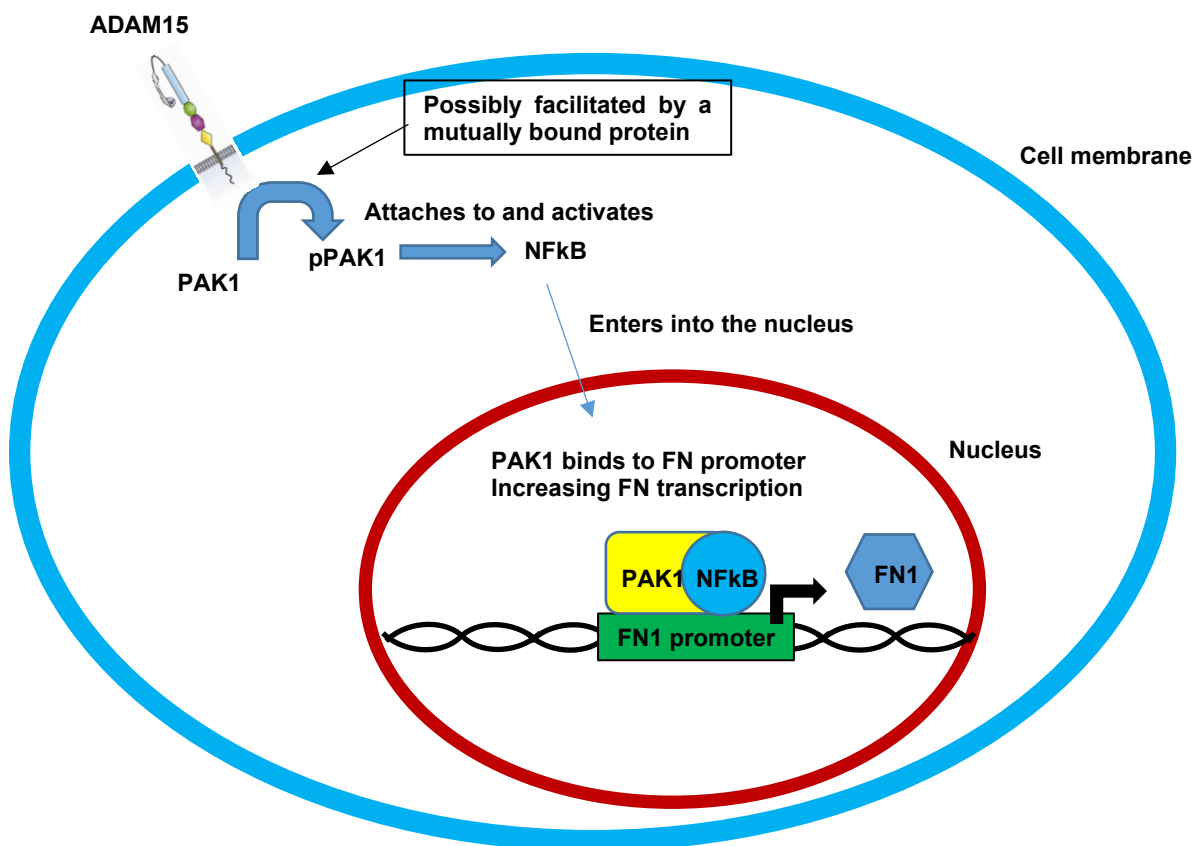


Figure 10. Schematic representation of ADAM15 interaction with PAK1 and and PAK1 regulation of fibronectin via PAK1-NF-kB-p65. Schematic showing how ADAM15 interacts with PAK1 and facilitates FN transcription.

The results described in this thesis show a novel role for ADAM15 in fibrosis. This mechanism could provide therapeutic implications for diseases characterized by an overabundance of fibrotic deposition such as idiopathic pulmonary fibrosis, liver cirrhosis, cardiovascular fibrosis, systemic sclerosis and nephritis.²⁰⁴ It may be possible to develop drugs to target the extracellular domain of ADAM15 and cause a conformational change in the protein structure so that the cytoplasmic tail is unavailable for interaction. Pharmacological inhibition of PAK1 has been shown to attenuate liver fibrosis in a mouse model by preventing myofibroblast activation.²⁰⁵ It also stands within reason that attenuating fibronectin secretion and polymerization would be beneficial in fibrotic disease by preventing fibroblast attachment and activation as has already been shown to be effective in mouse models of liver, heart and kidney disease.^{180, 206,}

207

Chapter 5

Limitations and Future Directions

5.1. Limitations

5.1.1. Disease model for heart failure

Using mouse models for heart failure studies is widely accepted. The models are advantageous because of the availability of genetically modified mice and greater litter size. In this research we used a chronic ligation of the LAD to model an ischemic insult. While this allows us to study the severity of post-MI remodeling, only 7% of patients are not treated with a reperfusion technique such as P-PCI.²⁰⁸ The chronic ligation model produces the most severe disease type, and this may mask other underlying mechanisms by which ADAM15 could act. This reason may explain why *Adam15*-deficiency did not alter the inflammatory response in a meaningful way, as the MI could be too severe to elucidate any nuanced inflammatory response. It is also possible that the way the tissue was harvested may affect the results. The infarcted, peri-infarcted, and non-infarcted regions of the heart are separated manually; therefore, it is feasible human error could factor into the results.

5.1.2. Ischemia models *in vitro*

The ischemia model used in this paper was adjusted from the oxygen glucose deprivation (OGD) model used to mimic ischemic conditions *in vitro*. This model deprives the cultured cells from glucose and oxygen (through the use of a hypoxic chamber) to affect the electron transport chain which causes cells to change their metabolic mechanism.²⁰⁹ Previous studies have shown this model to be viable for inducing an ischemia insult in cultured fibroblasts.^{210, 211} The issue with this model is that it isolates the cell from its natural environment. The

heart produces mechanical loads that fibroblasts are responsive to and in turn fibroblasts turn mechanical signals into biological events such as gene expression, including extracellular matrix proteins.²¹² Altered mechanical environment affects fibronectin gene expression in fibroblasts *in vivo* and *in vitro*.²¹³⁻²¹⁵ This may explain the differences seen in the above data where fibronectin was decreased in fibroblasts in the presence of an *in vitro* ischemic insult whereas fibronectin was increased in response to MI *in vivo*.

The OGD model also does not reflect cell-cell interactions. Cardiomyocytes and fibroblasts can interact in a number of ways including biochemical and biomechanical. A biochemical interaction between cardiomyocytes and fibroblasts involves TGF- β . The loss of TGF- β signalling in cardiomyocytes *in vivo* is sufficient to reduce fibrosis in a pressure overload rat model.²¹⁶ Another form of biochemical signaling that is relevant to MI is the effect of lactate on fibroblasts. Lactate is generated in response to a hypoxic environment and it was found that lactate acting on fibroblasts promoted the myofibroblast response.^{217, 218} Fibroblasts are the primary cell type that produce and secrete ECM products such as collagen and fibronectin. These ECM components can also be sensed by other cells such as cardiomyocytes.²¹⁹⁻²²² Excessive ECM production due to cardiac fibrosis can lead to impaired cardiomyocyte connectivity and function.²²³

In summary, the OGD single cell type model excels at looking at fibroblasts and how those fibroblasts respond to stimulus. However, it fails to take into account other factors at work that could influence how the fibroblasts

behave in a system and this may have unintended consequences on the results of experimentation.

5.2. Future directions

5.2.1. Role of ADAM15 in an ischemia/reperfusion model

Because of the aforementioned severity of MI induced by permanent ligation of the LAD, examining the role of ADAM15 in a less intense model may show that ADAM15 inhibition/deletion is beneficial for LV remodeling. As previously discussed, fibronectin plays an important role in myofibroblast transformation and fibrosis. In a I/R model, *Adam15* deletion could limit the extent of fibrosis and lead to better LV remodeling post-MI.

5.2.2. Elucidate sex differences in *Adam15*-deficient mice

We found stark differences in male and female *Adam15*^{-/-} mice responses to MI. The results are preliminary but female *Adam15*^{-/-} mice exhibited no LV rupture, and no decrease in the amount of LOX-1 present in post-MI hearts (Figure 11). This difference could be due to the actions of sex hormones and may aid in understanding the sex differences present in ischemic cardiomyopathies.

Estrogen was initially found to enhance the proliferation of cardiac fibroblasts, and in turn may affect ECM composition through the number of cardiac fibroblasts.²²⁴ However, it was found more recently that activation of

GPR30, a g-coupled receptor that responds to estrogen, prevented cardiac proliferation and fibrosis both *in vitro* and *in vivo*.²²⁵ Estrogen may also inhibit fibrosis through its actions on cardiac fibroblasts. Estrogen was found to prevent cardiac fibrosis by blocking the effects of angiotensin II and endothelin-1, two profibrotic molecules.²²⁶ In a transverse aortic constriction model of heart failure in male mice, exogenous estrogen administration was found to improve ejection fraction, cardiac hemodynamics, and reverse the fibrotic scarring observed in heart failure.²²⁷ One of the key mechanisms of this action is the stimulation of angiogenesis, as in the presence of an angiogenesis inhibitor estrogen failed to rescue heart failure.²²⁷ Estrogen can also inhibit IL-6 expression by inhibiting NFkB through the binding of estrogen receptor- α to NFkB, and by doing so can limit an inflammatory response.²¹ Estrogen may play a vital role in preventing the accumulation of cholesterol, thereby attenuating plaque formation and myocardial infarction.²² What may be occurring in female *Adam15*^{-/-} mice is that while loss of ADAM15 is deleterious to cardiac remodeling post-MI, the presence of estrogen may counteract that deleterious effect.

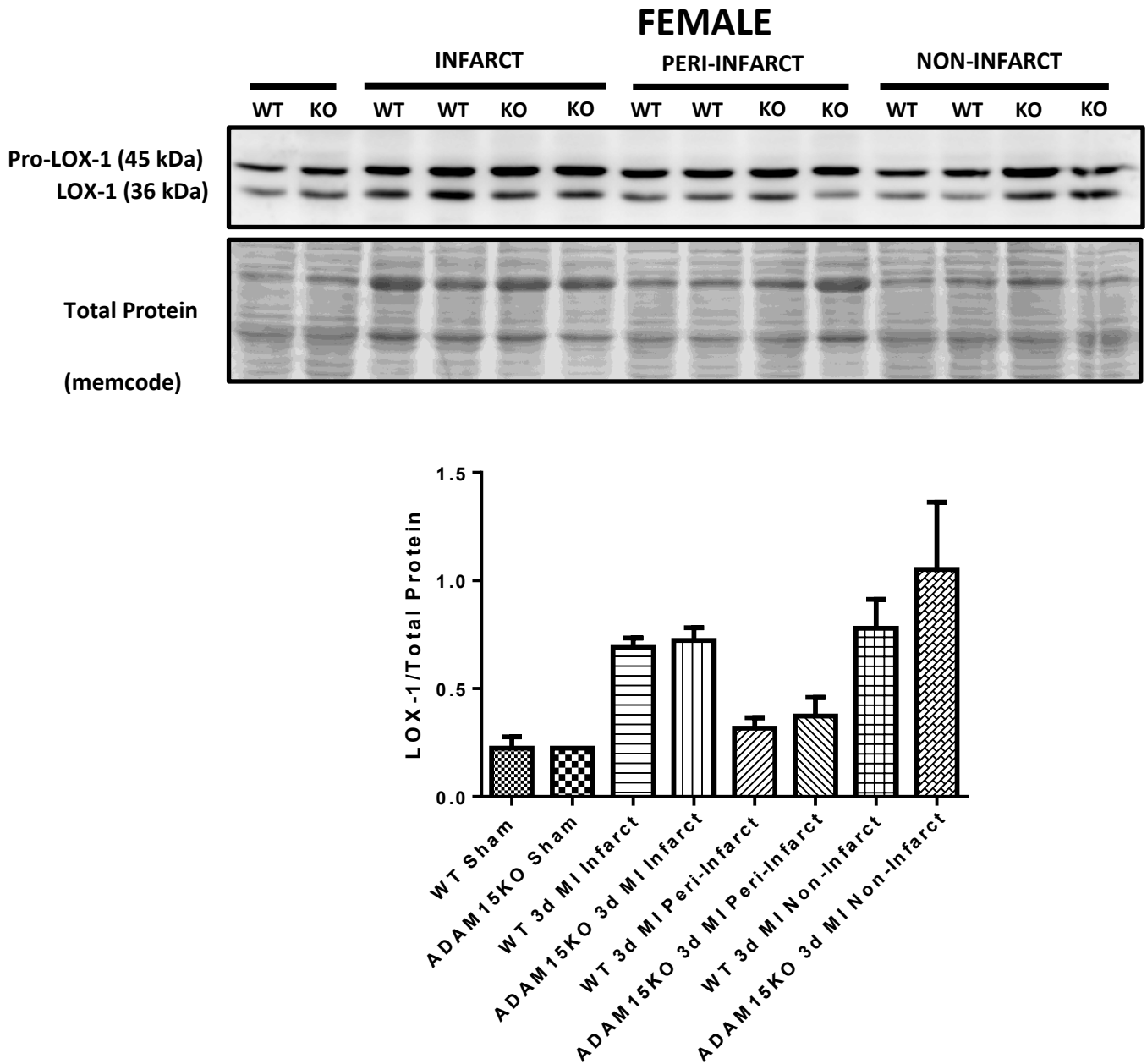


Figure 11. Loss of ADAM15 in female mice does not alter LOX-1 upregulation post-MI as compared to the female WT counterpart.

Representative immunoblot and quantification of LOX-1 in female *Adam15^{-/-}* post-MI. Averaged values represent Mean ± SEM.

References

1. Benjamin EJ, Muntner P, Alonso A, Bittencourt MS, Callaway CW, Carson AP, Chamberlain AM, Chang AR, Cheng S, Das SR, Delling FN, Djousse L, Elkind MSV, Ferguson JF, Fornage M, Jordan LC, Khan SS, Kissela BM, Knutson KL, Kwan TW, Lackland DT, Lewis TT, Lichtman JH, Longenecker CT, Loop MS, Lutsey PL, Martin SS, Matsushita K, Moran AE, Mussolino ME, O'Flaherty M, Pandey A, Perak AM, Rosamond WD, Roth GA, Sampson UKA, Satou GM, Schroeder EB, Shah SH, Spartano NL, Stokes A, Tirschwell DL, Tsao CW, Turakhia MP, VanWagner LB, Wilkins JT, Wong SS and Virani SS. Heart Disease and Stroke Statistics—2019 Update: A Report From the American Heart Association. *Circulation*. 2019;139:e56-e528.
2. Pinto AR, Ilinykh A, Ivey MJ, Kuwabara JT, D'Antoni ML, Debuque R, Chandran A, Wang L, Arora K, Rosenthal NA and Tallquist MD. Revisiting Cardiac Cellular Composition. *Circulation research*. 2016;118:400-409.
3. Argulian E, Sherrid MV and Messerli FH. Misconceptions and Facts About Hypertrophic Cardiomyopathy. *Am J Med*. 2016;129:148-52.
4. Branzi A, Romeo G, Specchia S, Lolli C, Binetti G, Devoto M, Bacchi M and Magnani B. Genetic heterogeneity of hypertrophic cardiomyopathy. *Int J Cardiol*. 1985;7:129-38.
5. Richard P, Charron P, Carrier L, Ledeuil C, Cheav T, Pichereau C, Benaiche A, Isnard R, Dubourg O, Burbanc M, Gueffet JP, Millaire A, Desnos M, Schwartz K, Hainque B and Komajda M. Hypertrophic cardiomyopathy: distribution of disease genes, spectrum of mutations, and implications for a molecular diagnosis strategy. *Circulation*. 2003;107:2227-32.
6. Toepfer CN, Wakimoto H, Garfinkel AC, McDonough B, Liao D, Jiang J, Tai AC, Gorham JM, Lunde IG, Lun M, Lynch TL, McNamara JW, Sadayappan S, Redwood CS, Watkins HC, Seidman JG and Seidman CE. Hypertrophic cardiomyopathy mutations in MYBPC3 dysregulate myosin. *Science Translational Medicine*. 2019;11:eaat1199.
7. Herman DS, Lam L, Taylor MR, Wang L, Teekakirikul P, Christodoulou D, Conner L, DePalma SR, McDonough B, Sparks E, Teodorescu DL, Cirino AL, Banner NR, Pennell DJ, Graw S, Merlo M, Di Lenarda A, Sinagra G, Bos JM, Ackerman MJ, Mitchell RN, Murry CE, Lakdawala NK, Ho CY, Barton PJ, Cook SA, Mestroni L, Seidman JG and Seidman CE. Truncations of titin causing dilated cardiomyopathy. *N Engl J Med*. 2012;366:619-28.
8. Parks SB, Kushner JD, Nauman D, Burgess D, Ludwigsen S, Peterson A, Li D, Jakobs P, Litt M, Porter CB, Rahko PS and Hershberger RE. Lamin A/C mutation analysis in a cohort of 324 unrelated patients with idiopathic or familial dilated cardiomyopathy. *Am Heart J*. 2008;156:161-9.
9. Jefferies JL, Eidem BW, Belmont JW, Craigen WJ, Ware SM, Fernbach SD, Neish SR, Smith EO and Towbin JA. Genetic predictors and remodeling of dilated cardiomyopathy in muscular dystrophy. *Circulation*. 2005;112:2799-804.
10. Burkett EL and Hershberger RE. Clinical and genetic issues in familial dilated cardiomyopathy. *J Am Coll Cardiol*. 2005;45:969-81.
11. Ervasti JM and Campbell KP. A role for the dystrophin-glycoprotein complex as a transmembrane linker between laminin and actin. *J Cell Biol*. 1993;122:809-23.
12. Nakamura A, Yoshida K, Fukushima K, Ueda H, Urasawa N, Koyama J, Yazaki Y, Yazaki M, Sakai T, Haruta S, Takeda S and Ikeda S. Follow-up of three patients with

a large in-frame deletion of exons 45-55 in the Duchenne muscular dystrophy (DMD) gene. *J Clin Neurosci*. 2008;15:757-63.

13. Ozawa E, Hagiwara Y and Yoshida M. Creatine kinase, cell membrane and Duchenne muscular dystrophy. *Mol Cell Biochem*. 1999;190:143-51.
14. Khera AV, Emdin CA, Drake I, Natarajan P, Bick AG, Cook NR, Chasman DI, Baber U, Mehran R, Rader DJ, Fuster V, Boerwinkle E, Melander O, Orho-Melander M, Ridker PM and Kathiresan S. Genetic Risk, Adherence to a Healthy Lifestyle, and Coronary Disease. *New England Journal of Medicine*. 2016;375:2349-2358.
15. Canada PHAo. Report from the Canadian Chronic Disease Surveillance System: Heart Disease in Canada. 2018.
16. Kannel WB, Hjortland MC, McNamara PM and Gordon T. Menopause and risk of cardiovascular disease: the Framingham study. *Annals of internal medicine*. 1976;85:447-52.
17. Vitale C, Fini M, Speziale G and Chierchia S. Gender differences in the cardiovascular effects of sex hormones. *Fundamental & clinical pharmacology*. 2010;24:675-85.
18. Kannel WB and Wilson PW. Risk factors that attenuate the female coronary disease advantage. *Archives of internal medicine*. 1995;155:57-61.
19. Bairey Merz CN, Johnson BD, Sharaf BL, Bittner V, Berga SL, Braunstein GD, Hodgson TK, Matthews KA, Pepine CJ, Reis SE, Reichel N, Rogers WJ, Pohost GM, Kelsey SF and Sopko G. Hypoestrogenemia of hypothalamic origin and coronary artery disease in premenopausal women: a report from the NHLBI-sponsored WISE study. *J Am Coll Cardiol*. 2003;41:413-9.
20. Villa A, Della Torre S, Stell A, Cook J, Brown M and Maggi A. Tetradian oscillation of estrogen receptor α is necessary to prevent liver lipid deposition. *Proc Natl Acad Sci U S A*. 2012;109:11806-11.
21. Galien R and Garcia T. Estrogen receptor impairs interleukin-6 expression by preventing protein binding on the NF-kappaB site. *Nucleic Acids Res*. 1997;25:2424-9.
22. Linton MF, Yancey PG, Davies SS, Jerome WG, Linton EF, Song WL, Doran AC and Vickers KC. The Role of Lipids and Lipoproteins in Atherosclerosis. In: K. R. Feingold, B. Anawalt, A. Boyce, G. Chrousos, W. W. de Herder, K. Dungan, A. Grossman, J. M. Hershman, H. J. Hofland, G. Kaltsas, C. Koch, P. Kopp, M. Korbonits, R. McLachlan, J. E. Morley, M. New, J. Purnell, F. Singer, C. A. Stratakis, D. L. Trencle and D. P. Wilson, eds. *Endotext* South Dartmouth (MA): MDText.com, Inc.

Copyright © 2000-2020, MDText.com, Inc.; 2000.

23. Mehta LS, Beckie TM, DeVon HA, Grines CL, Krumholz HM, Johnson MN, Lindley KJ, Vaccarino V, Wang TY, Watson KE and Wenger NK. Acute Myocardial Infarction in Women. *Circulation*. 2016;133:916-947.
24. Khan NA, Daskalopoulou SS, Karp I, Eisenberg MJ, Pelletier R, Tsadok MA, Dasgupta K, Norris CM and Pilote L. Sex differences in acute coronary syndrome symptom presentation in young patients. *JAMA internal medicine*. 2013;173:1863-71.
25. McMechan SR and Adgey AA. Age related outcome in acute myocardial infarction. Elderly people benefit from thrombolysis and should be included in trials. *BMJ*. 1998;317:1334-1335.
26. Relationship of blood pressure, serum cholesterol, smoking habit, relative weight and ECG abnormalities to incidence of major coronary events: final report of the pooling project. The pooling project research group. *Journal of chronic diseases*. 1978;31:201-306.

27. Oparil S, Acelajado MC, Bakris GL, Berlowitz DR, Cifková R, Dominiczak AF, Grassi G, Jordan J, Poulter NR, Rodgers A and Whelton PK. Hypertension. *Nat Rev Dis Primers*. 2018;4:18014-18014.
28. Reindl M, Reinstadler SJ, Feistritzer HJ, Theurl M, Basic D, Eigler C, Holzknecht M, Mair J, Mayr A, Klug G and Metzler B. Relation of Low-Density Lipoprotein Cholesterol With Microvascular Injury and Clinical Outcome in Revascularized ST-Elevation Myocardial Infarction. *J Am Heart Assoc*. 2017;6.
29. Jiao Z-Y, Li X-T, Li Y-B, Zheng M-L, Cai J, Chen S-H, Wu S-L and Yang X-C. Correlation of triglycerides with myocardial infarction and analysis of risk factors for myocardial infarction in patients with elevated triglyceride. *J Thorac Dis*. 2018;10:2551-2557.
30. Poirier P, Giles TD, Bray GA, Hong Y, Stern JS, Pi-Sunyer FX and Eckel RH. Obesity and Cardiovascular Disease: Pathophysiology, Evaluation, and Effect of Weight Loss. *Circulation*. 2006;113:898-918.
31. Jacoby RM and Nesto RW. Acute myocardial infarction in the diabetic patient: pathophysiology, clinical course and prognosis. *Journal of the American College of Cardiology*. 1992;20:736-44.
32. Kaur J. A comprehensive review on metabolic syndrome. *Cardiol Res Pract*. 2014;2014:943162-943162.
33. Myocardial Infarction Genetics C, Kathiresan S, Voight BF, Purcell S, Musunuru K, Ardissino D, Mannucci PM, Anand S, Engert JC, Samani NJ, Schunkert H, Erdmann J, Reilly MP, Rader DJ, Morgan T, Spertus JA, Stoll M, Girelli D, McKeown PP, Patterson CC, Siscovick DS, O'Donnell CJ, Elosua R, Peltonen L, Salomaa V, Schwartz SM, Melander O, Altshuler D, Ardissino D, Merlini PA, Berzuini C, Bernardinelli L, Peyvandi F, Tubaro M, Celli P, Ferrario M, Fève R, Marziliano N, Casari G, Galli M, Ribichini F, Rossi M, Bernardi F, Zonzin P, Piazza A, Mannucci PM, Schwartz SM, Siscovick DS, Yee J, Friedlander Y, Elosua R, Marrugat J, Lucas G, Subirana I, Sala J, Ramos R, Kathiresan S, Meigs JB, Williams G, Nathan DM, MacRae CA, O'Donnell CJ, Salomaa V, Havulinna AS, Peltonen L, Melander O, Berglund G, Voight BF, Kathiresan S, Hirschhorn JN, Asselta R, Duga S, Sreafico M, Musunuru K, Daly MJ, Purcell S, Voight BF, Purcell S, Nemesh J, Korn JM, McCarroll SA, Schwartz SM, Yee J, Kathiresan S, Lucas G, Subirana I, Elosua R, Surti A, Guiducci C, Gianniny L, Mirel D, Parkin M, Burt N, Gabriel SB, Samani NJ, Thompson JR, Braund PS, Wright BJ, Balmforth AJ, Ball SG, Hall AS, Wellcome Trust Case Control C, Schunkert H, Erdmann J, Linsel-Nitschke P, Lieb W, Ziegler A, König I, Hengstenberg C, Fischer M, Stark K, Grosshennig A, Preuss M, Wichmann HE, Schreiber S, Schunkert H, Samani NJ, Erdmann J, Ouwehand W, Hengstenberg C, Deloukas P, Scholz M, Cambien F, Reilly MP, Li M, Chen Z, Wilensky R, Matthai W, Qasim A, Hakonarson HH, Devaney J, Burnett M-S, Pichard AD, Kent KM, Satler L, Lindsay JM, Waksman R, Knouff CW, Waterworth DM, Walker MC, Mooser V, Epstein SE, Rader DJ, Scheffold T, Berger K, Stoll M, Häge A, Girelli D, Martinelli N, Olivieri O, Corrocher R, Morgan T, Spertus JA, McKeown P, Patterson CC, Schunkert H, Erdmann E, Linsel-Nitschke P, Lieb W, Ziegler A, König IR, Hengstenberg C, Fischer M, Stark K, Grosshennig A, Preuss M, Wichmann HE, Schreiber S, Hólm H, Thorleifsson G, Thorsteinsdóttir U, Stefansson K, Engert JC, Do R, Xie C, Anand S, Kathiresan S, Ardissino D, Mannucci PM, Siscovick D, O'Donnell CJ, Samani NJ, Melander O, Elosua R, Peltonen L, Salomaa V, Schwartz SM and Altshuler D. Genome-wide association of early-onset myocardial infarction with single nucleotide polymorphisms and copy number variants. *Nat Genet*. 2009;41:334-341.
34. Arnaout R, Nah G, Marcus G, Tseng Z, Foster E, Harris IS, Divanji P, Klein L, Gonzalez J and Parikh N. Pregnancy complications and premature cardiovascular events among 1.6 million California pregnancies. *Open heart*. 2019;6:e000927.

35. Chung WS, Lin CL, Peng CL, Chen YF, Lu CC, Sung FC and Kao CH. Rheumatoid arthritis and risk of acute myocardial infarction--a nationwide retrospective cohort study. *International journal of cardiology*. 2013;168:4750-4.
36. Rangel A, Lavallo C, Chávez E, Jiménez M, Acosta JL, Baduí E and Albarrán H. Myocardial infarction in patients with systemic lupus erythematosus with normal findings from coronary arteriography and without coronary vasculitis--case reports. *Angiology*. 1999;50:245-53.
37. Eltzschig HK and Eckle T. Ischemia and reperfusion--from mechanism to translation. *Nature medicine*. 2011;17:1391-401.
38. Timmers L, Pasterkamp G, de Hoog VC, Arslan F, Appelman Y and de Kleijn DP. The innate immune response in reperfused myocardium. *Cardiovasc Res*. 2012;94:276-83.
39. Scaffidi P, Misteli T and Bianchi ME. Release of chromatin protein HMGB1 by necrotic cells triggers inflammation. *Nature*. 2002;418:191-5.
40. Frangogiannis NG. Interleukin-1 in cardiac injury, repair, and remodeling: pathophysiologic and translational concepts. *Discoveries (Craiova)*. 2015;3:e41.
41. Tian M, Yuan Y-C, Li J-Y, Gionfriddo MR and Huang R-C. Tumor necrosis factor- α and its role as a mediator in myocardial infarction: A brief review. *Chronic Dis Transl Med*. 2015;1:18-26.
42. Ritschel VN, Seljeflot I, Arnesen H, Halvorsen S, Weiss T, Eritsland J and Andersen GØ. IL-6 signalling in patients with acute ST-elevation myocardial infarction. *Results Immunol*. 2013;4:8-13.
43. O'Brien LC, Mezzaroma E, Van Tassell BW, Marchetti C, Carbone S, Abbate A and Toldo S. Interleukin-18 as a therapeutic target in acute myocardial infarction and heart failure. *Mol Med*. 2014;20:221-229.
44. Fiordelisi A, Iaccarino G, Morisco C, Coscioni E and Sorriento D. NFkappaB is a Key Player in the Crosstalk between Inflammation and Cardiovascular Diseases. *Int J Mol Sci*. 2019;20:1599.
45. Gordon JW, Shaw JA and Kirshenbaum LA. Multiple facets of NF- κ B in the heart: to be or not to NF- κ B. *Circ Res*. 2011;108:1122-32.
46. Hayden MS and Ghosh S. Signaling to NF- κ B. *Genes & development*. 2004;18:2195-224.
47. Khodayari S, Khodayari H, Amiri AZ, Eslami M, Farhud D, Hescheler J and Nayernia K. Inflammatory Microenvironment of Acute Myocardial Infarction Prevents Regeneration of Heart with Stem Cells Therapy. *Cellular physiology and biochemistry : international journal of experimental cellular physiology, biochemistry, and pharmacology*. 2019;53:887-909.
48. Kobayashi Y. Neutrophil infiltration and chemokines. *Critical reviews in immunology*. 2006;26:307-16.
49. Bujak M, Dobaczewski M, Chatila K, Mendoza LH, Li N, Reddy A and Frangogiannis NG. Interleukin-1 receptor type I signaling critically regulates infarct healing and cardiac remodeling. *Am J Pathol*. 2008;173:57-67.
50. Maekawa N, Wada H, Kanda T, Niwa T, Yamada Y, Saito K, Fujiwara H, Sekikawa K and Seishima M. Improved myocardial ischemia/reperfusion injury in mice lacking tumor necrosis factor- α . *Journal of the American College of Cardiology*. 2002;39:1229-35.
51. Liehn EA, Piccinini AM, Koenen RR, Soehnlein O, Adage T, Fatu R, Curaj A, Popescu A, Zerneck A, Kungl AJ and Weber C. A new monocyte chemotactic protein-1/chemokine CC motif ligand-2 competitor limiting neointima formation and myocardial ischemia/reperfusion injury in mice. *Journal of the American College of Cardiology*. 2010;56:1847-57.

52. Dewald O, Zymek P, Winkelmann K, Koerting A, Ren G, Abou-Khamis T, Michael LH, Rollins BJ, Entman ML and Frangogiannis NG. CCL2/Monocyte Chemoattractant Protein-1 regulates inflammatory responses critical to healing myocardial infarcts. *Circ Res*. 2005;96:881-9.
53. Hayasaki T, Kaikita K, Okuma T, Yamamoto E, Kuziel WA, Ogawa H and Takeya M. CC chemokine receptor-2 deficiency attenuates oxidative stress and infarct size caused by myocardial ischemia-reperfusion in mice. *Circ J*. 2006;70:342-51.
54. Kaikita K, Hayasaki T, Okuma T, Kuziel WA, Ogawa H and Takeya M. Targeted deletion of CC chemokine receptor 2 attenuates left ventricular remodeling after experimental myocardial infarction. *Am J Pathol*. 2004;165:439-47.
55. Kukielka GL, Hawkins HK, Michael L, Manning AM, Youker K, Lane C, Entman ML, Smith CW and Anderson DC. Regulation of intercellular adhesion molecule-1 (ICAM-1) in ischemic and reperfused canine myocardium. *J Clin Invest*. 1993;92:1504-16.
56. Gwechenberger M, Mendoza LH, Youker KA, Frangogiannis NG, Smith CW, Michael LH and Entman ML. Cardiac myocytes produce interleukin-6 in culture and in viable border zone of reperfused infarctions. *Circulation*. 1999;99:546-51.
57. Tarzami ST, Cheng R, Miao W, Kitsis RN and Berman JW. Chemokine expression in myocardial ischemia: MIP-2 dependent MCP-1 expression protects cardiomyocytes from cell death. *J Mol Cell Cardiol*. 2002;34:209-21.
58. Zhu M, Goetsch SC, Wang Z, Luo R, Hill JA, Schneider J, Morris SM, Jr. and Liu ZP. FoxO4 promotes early inflammatory response upon myocardial infarction via endothelial Arg1. *Circ Res*. 2015;117:967-77.
59. Chukwuemeka AO, Brown KA, Venn GE and Chambers DJ. Changes in P-selectin expression on cardiac microvessels in blood-perfused rat hearts subjected to ischemia-reperfusion. *The Annals of thoracic surgery*. 2005;79:204-11.
60. Weyrich AS, Ma XY, Lefer DJ, Albertine KH and Lefer AM. In vivo neutralization of P-selectin protects feline heart and endothelium in myocardial ischemia and reperfusion injury. *J Clin Invest*. 1993;91:2620-9.
61. Yoshida M, Takano Y, Sasaoka T, Izumi T and Kimura A. E-selectin polymorphism associated with myocardial infarction causes enhanced leukocyte-endothelial interactions under flow conditions. *Arteriosclerosis, thrombosis, and vascular biology*. 2003;23:783-8.
62. Kolaczowska E and Kubes P. Neutrophil recruitment and function in health and inflammation. *Nature reviews Immunology*. 2013;13:159-75.
63. Kumar AG, Ballantyne CM, Michael LH, Kukielka GL, Youker KA, Lindsey ML, Hawkins HK, Birdsall HH, MacKay CR, LaRosa GJ, Rossen RD, Smith CW and Entman ML. Induction of monocyte chemoattractant protein-1 in the small veins of the ischemic and reperfused canine myocardium. *Circulation*. 1997;95:693-700.
64. Frangogiannis NG, Mendoza LH, Lewallen M, Michael LH, Smith CW and Entman ML. Induction and suppression of interferon-inducible protein 10 in reperfused myocardial infarcts may regulate angiogenesis. *FASEB J*. 2001;15:1428-30.
65. Yan X, Anzai A, Katsumata Y, Matsuhashi T, Ito K, Endo J, Yamamoto T, Takeshima A, Shinmura K, Shen W, Fukuda K and Sano M. Temporal dynamics of cardiac immune cell accumulation following acute myocardial infarction. *J Mol Cell Cardiol*. 2013;62:24-35.
66. Mantovani A, Cassatella MA, Costantini C and Jaillon S. Neutrophils in the activation and regulation of innate and adaptive immunity. *Nature reviews Immunology*. 2011;11:519-31.

67. Serhan CN, Chiang N and Van Dyke TE. Resolving inflammation: dual anti-inflammatory and pro-resolution lipid mediators. *Nature reviews Immunology*. 2008;8:349-361.
68. Soehnlein O and Lindbom L. Phagocyte partnership during the onset and resolution of inflammation. *Nature reviews Immunology*. 2010;10:427-39.
69. Herter J and Zarbock A. Integrin Regulation during Leukocyte Recruitment. *J Immunol*. 2013;190:4451-7.
70. Wang S, Voisin MB, Larbi KY, Dangerfield J, Scheiermann C, Tran M, Maxwell PH, Sorokin L and Nourshargh S. Venular basement membranes contain specific matrix protein low expression regions that act as exit points for emigrating neutrophils. *The Journal of experimental medicine*. 2006;203:1519-32.
71. Phillipson M, Heit B, Colarusso P, Liu L, Ballantyne CM and Kubes P. Intraluminal crawling of neutrophils to emigration sites: a molecularly distinct process from adhesion in the recruitment cascade. *The Journal of experimental medicine*. 2006;203:2569-75.
72. Proebstl D, Voisin MB, Woodfin A, Whiteford J, D'Acquisto F, Jones GE, Rowe D and Nourshargh S. Pericytes support neutrophil subendothelial cell crawling and breaching of venular walls in vivo. *The Journal of experimental medicine*. 2012;209:1219-34.
73. Williams MR, Azcutia V, Newton G, Alcaide P and Luscinskas FW. Emerging mechanisms of neutrophil recruitment across endothelium. *Trends Immunol*. 2011;32:461-9.
74. Puhl S-L and Steffens S. Neutrophils in Post-myocardial Infarction Inflammation: Damage vs. Resolution? *Front Cardiovasc Med*. 2019;6:25-25.
75. Boufenzler A, Lemarié J, Simon T, Derive M, Bouazza Y, Tran N, Maskali F, Groubatch F, Bonnin P, Bastien C, Bruneval P, Marie PY, Cohen R, Danchin N, Silvestre JS, Ait-Oufella H and Gibot S. TREM-1 Mediates Inflammatory Injury and Cardiac Remodeling Following Myocardial Infarction. *Circ Res*. 2015;116:1772-82.
76. Simpson PJ, Todd RF, 3rd, Fantone JC, Mickelson JK, Griffin JD and Lucchesi BR. Reduction of experimental canine myocardial reperfusion injury by a monoclonal antibody (anti-Mo1, anti-CD11b) that inhibits leukocyte adhesion. *J Clin Invest*. 1988;81:624-9.
77. Entman ML, Youker K, Shoji T, Kukielka G, Shappell SB, Taylor AA and Smith CW. Neutrophil induced oxidative injury of cardiac myocytes. A compartmented system requiring CD11b/CD18-ICAM-1 adherence. *J Clin Invest*. 1992;90:1335-45.
78. Swirski FK, Nahrendorf M, Etzrodt M, Wildgruber M, Cortez-Retamozo V, Panizzi P, Figueiredo JL, Kohler RH, Chudnovskiy A, Waterman P, Aikawa E, Mempel TR, Libby P, Weissleder R and Pittet MJ. Identification of splenic reservoir monocytes and their deployment to inflammatory sites. *Science*. 2009;325:612-6.
79. Dick SA, Macklin JA, Nejat S, Momen A, Clemente-Casares X, Althagafi MG, Chen J, Kantores C, Hosseinzadeh S, Aronoff L, Wong A, Zaman R, Barbu I, Besla R, Lavine KJ, Razani B, Ginhoux F, Husain M, Cybulsky MI, Robbins CS and Epelman S. Self-renewing resident cardiac macrophages limit adverse remodeling following myocardial infarction. *Nat Immunol*. 2019;20:29-39.
80. Shinde AV and Frangogiannis NG. Fibroblasts in myocardial infarction: a role in inflammation and repair. *J Mol Cell Cardiol*. 2014;70:74-82.
81. Saxena A, Chen W, Su Y, Rai V, Uche OU, Li N and Frangogiannis NG. IL-1 induces proinflammatory leukocyte infiltration and regulates fibroblast phenotype in the infarcted myocardium. *J Immunol*. 2013;191:4838-48.

82. Trial J, Baughn RE, Wygant JN, McIntyre BW, Birdsall HH, Youker KA, Evans A, Entman ML and Rossen RD. Fibronectin fragments modulate monocyte VLA-5 expression and monocyte migration. *J Clin Invest.* 1999;104:419-30.
83. Dobaczewski M, Gonzalez-Quesada C and Frangogiannis NG. The extracellular matrix as a modulator of the inflammatory and reparative response following myocardial infarction. *J Mol Cell Cardiol.* 2010;48:504-11.
84. Rienks M, Papageorgiou AP, Frangogiannis NG and Heymans S. Myocardial extracellular matrix: an ever-changing and diverse entity. *Circ Res.* 2014;114:872-88.
85. Geering B, Stoeckle C, Conus S and Simon HU. Living and dying for inflammation: neutrophils, eosinophils, basophils. *Trends Immunol.* 2013;34:398-409.
86. Horckmans M, Ring L, Duchene J, Santovito D, Schloss MJ, Drechsler M, Weber C, Soehnlein O and Steffens S. Neutrophils orchestrate post-myocardial infarction healing by polarizing macrophages towards a reparative phenotype. *European heart journal.* 2017;38:187-197.
87. Nahrendorf M, Swirski FK, Aikawa E, Stangenberg L, Wurdinger T, Figueiredo JL, Libby P, Weissleder R and Pittet MJ. The healing myocardium sequentially mobilizes two monocyte subsets with divergent and complementary functions. *The Journal of experimental medicine.* 2007;204:3037-47.
88. Nahrendorf M, Pittet MJ and Swirski FK. Monocytes: protagonists of infarct inflammation and repair after myocardial infarction. *Circulation.* 2010;121:2437-45.
89. Hanna A and Frangogiannis NG. The Role of the TGF- β Superfamily in Myocardial Infarction. *Front Cardiovasc Med.* 2019;6:140-140.
90. Dobaczewski M, Chen W and Frangogiannis NG. Transforming growth factor (TGF)- β signaling in cardiac remodeling. *J Mol Cell Cardiol.* 2011;51:600-6.
91. Gombozhapova A, Rogovskaya Y, Shurupov V, Rebenkova M, Kzhyshkowska J, Popov SV, Karpov RS and Ryabov V. Macrophage activation and polarization in post-infarction cardiac remodeling. *J Biomed Sci.* 2017;24:13-13.
92. Barbay V, Houssari M, Mekki M, Banquet S, Edwards-Lévy F, Henry JP, Dumesnil A, Adriouch S, Thuillez C, Richard V and Brakenhielm E. Role of M2-like macrophage recruitment during angiogenic growth factor therapy. *Angiogenesis.* 2015;18:191-200.
93. Ferraro B, Leoni G, Hinkel R, Ormanns S, Paulin N, Ortega-Gomez A, Viola JR, de Jong R, Bongiovanni D, Bozoglu T, Maas SL, D'Amico M, Kessler T, Zeller T, Hristov M, Reutelingsperger C, Sager HB, Döring Y, Nahrendorf M, Kupatt C and Soehnlein O. Pro-Angiogenic Macrophage Phenotype to Promote Myocardial Repair. *Journal of the American College of Cardiology.* 2019;73:2990.
94. Ren G, Michael LH, Entman ML and Frangogiannis NG. Morphological characteristics of the microvasculature in healing myocardial infarcts. *The journal of histochemistry and cytochemistry : official journal of the Histochemistry Society.* 2002;50:71-9.
95. Zymek P, Bujak M, Chatila K, Cieslak A, Thakker G, Entman ML and Frangogiannis NG. The role of platelet-derived growth factor signaling in healing myocardial infarcts. *Journal of the American College of Cardiology.* 2006;48:2315-23.
96. Chen CW, Okada M, Proto JD, Gao X, Sekiya N, Beckman SA, Corselli M, Crisan M, Saporov A, Tobita K, Péault B and Huard J. Human pericytes for ischemic heart repair. *Stem cells (Dayton, Ohio).* 2013;31:305-16.
97. Katare R, Riu F, Mitchell K, Gubernator M, Campagnolo P, Cui Y, Fortunato O, Avolio E, Cesselli D, Beltrami AP, Angelini G, Emanuelli C and Madeddu P. Transplantation of human pericyte progenitor cells improves the repair of infarcted heart through activation of an angiogenic program involving micro-RNA-132. *Circ Res.* 2011;109:894-906.

98. Santiago JJ, Dangerfield AL, Rattan SG, Bathe KL, Cunnington RH, Raizman JE, Bedosky KM, Freed DH, Kardami E and Dixon IM. Cardiac fibroblast to myofibroblast differentiation in vivo and in vitro: expression of focal adhesion components in neonatal and adult rat ventricular myofibroblasts. *Developmental dynamics : an official publication of the American Association of Anatomists*. 2010;239:1573-84.
99. Frangogiannis NG, Michael LH and Entman ML. Myofibroblasts in reperfused myocardial infarcts express the embryonic form of smooth muscle myosin heavy chain (SMemb). *Cardiovasc Res*. 2000;48:89-100.
100. Willems IE, Havenith MG, De Mey JG and Daemen MJ. The alpha-smooth muscle actin-positive cells in healing human myocardial scars. *Am J Pathol*. 1994;145:868-75.
101. Turner NA and Porter KE. Function and fate of myofibroblasts after myocardial infarction. *Fibrogenesis & tissue repair*. 2013;6:5.
102. Yano T, Miura T, Ikeda Y, Matsuda E, Saito K, Miki T, Kobayashi H, Nishino Y, Ohtani S and Shimamoto K. Intracardiac fibroblasts, but not bone marrow derived cells, are the origin of myofibroblasts in myocardial infarct repair. *Cardiovascular pathology : the official journal of the Society for Cardiovascular Pathology*. 2005;14:241-6.
103. Möllmann H, Nef HM, Kostin S, von Kalle C, Pilz I, Weber M, Schaper J, Hamm CW and Elsässer A. Bone marrow-derived cells contribute to infarct remodelling. *Cardiovasc Res*. 2006;71:661-71.
104. Zeisberg EM, Tarnavski O, Zeisberg M, Dorfman AL, McMullen JR, Gustafsson E, Chandraker A, Yuan X, Pu WT, Roberts AB, Neilson EG, Sayegh MH, Izumo S and Kalluri R. Endothelial-to-mesenchymal transition contributes to cardiac fibrosis. *Nature medicine*. 2007;13:952-61.
105. Hinz B, Phan SH, Thannickal VJ, Galli A, Bochaton-Piallat ML and Gabbiani G. The myofibroblast: one function, multiple origins. *Am J Pathol*. 2007;170:1807-16.
106. Arslan F, Smeets MB, Riem Vis PW, Karper JC, Quax PH, Bongartz LG, Peters JH, Hofer IE, Doevendans PA, Pasterkamp G and de Kleijn DP. Lack of fibronectin-EDA promotes survival and prevents adverse remodeling and heart function deterioration after myocardial infarction. *Circ Res*. 2011;108:582-92.
107. Dobaczewski M, Bujak M, Li N, Gonzalez-Quesada C, Mendoza LH, Wang XF and Frangogiannis NG. Smad3 signaling critically regulates fibroblast phenotype and function in healing myocardial infarction. *Circ Res*. 2010;107:418-28.
108. Thodeti CK, Paruchuri S and Meszaros JG. A TRP to cardiac fibroblast differentiation. *Channels (Austin, Tex)*. 2013;7:211-4.
109. Davis J, Burr AR, Davis GF, Birnbaumer L and Molkentin JD. A TRPC6-dependent pathway for myofibroblast transdifferentiation and wound healing in vivo. *Developmental cell*. 2012;23:705-15.
110. Dobaczewski M, Bujak M, Zymek P, Ren G, Entman ML and Frangogiannis NG. Extracellular matrix remodeling in canine and mouse myocardial infarcts. *Cell Tissue Res*. 2006;324:475-88.
111. Frangogiannis NG. Matricellular proteins in cardiac adaptation and disease. *Physiol Rev*. 2012;92:635-88.
112. González-Santamaría J, Villalba M, Busnadiego O, López-Olañeta MM, Sandoval P, Snabel J, López-Cabrera M, Erler JT, Hanemaaijer R, Lara-Pezzi E and Rodríguez-Pascual F. Matrix cross-linking lysyl oxidases are induced in response to myocardial infarction and promote cardiac dysfunction. *Cardiovasc Res*. 2016;109:67-78.
113. Fogelgren B, Polgár N, Szauter KM, Ujfaludi Z, Laczkó R, Fong KS and Csiszar K. Cellular fibronectin binds to lysyl oxidase with high affinity and is critical for its proteolytic activation. *The Journal of biological chemistry*. 2005;280:24690-7.

114. Heineke J and Molkentin JD. Regulation of cardiac hypertrophy by intracellular signalling pathways. *Nat Rev Mol Cell Biol.* 2006;7:589-600.
115. Weber KT, Sun Y, Bhattacharya SK, Ahokas RA and Gerling IC. Myofibroblast-mediated mechanisms of pathological remodelling of the heart. *Nature reviews Cardiology.* 2013;10:15-26.
116. van den Borne SW, Diez J, Blankesteyn WM, Verjans J, Hofstra L and Narula J. Myocardial remodeling after infarction: the role of myofibroblasts. *Nature reviews Cardiology.* 2010;7:30-7.
117. Chute M, Aujla P, Jana S and Kassiri Z. The Non-Fibrillar Side of Fibrosis: Contribution of the Basement Membrane, Proteoglycans, and Glycoproteins to Myocardial Fibrosis. *Journal of cardiovascular development and disease.* 2019;6.
118. Kohan M, Muro AF, White ES and Berkman N. EDA-containing cellular fibronectin induces fibroblast differentiation through binding to alpha4beta7 integrin receptor and MAPK/Erk 1/2-dependent signaling. *FASEB J.* 2010;24:4503-4512.
119. Thannickal VJ, Lee DY, White ES, Cui Z, Larios JM, Chacon R, Horowitz JC, Day RM and Thomas PE. Myofibroblast differentiation by transforming growth factor-beta1 is dependent on cell adhesion and integrin signaling via focal adhesion kinase. *The Journal of biological chemistry.* 2003;278:12384-9.
120. Gabbiani G. The myofibroblast in wound healing and fibrocontractive diseases. *The Journal of pathology.* 2003;200:500-3.
121. Ulrich MM, Janssen AM, Daemen MJ, Rappaport L, Samuel JL, Contard F, Smits JF and Cleutjens JP. Increased expression of fibronectin isoforms after myocardial infarction in rats. *J Mol Cell Cardiol.* 1997;29:2533-43.
122. Valiente-Alandi I, Potter Sarah J, Salvador Ane M, Schafer Allison E, Schips T, Carrillo-Salinas F, Gibson Aaron M, Nieman Michelle L, Perkins C, Sargent Michelle A, Huo J, Lorenz John N, DeFalco T, Molkentin Jeffery D, Alcaide P and Blaxall Burns C. Inhibiting Fibronectin Attenuates Fibrosis and Improves Cardiac Function in a Model of Heart Failure. *Circulation.* 2018;138:1236-1252.
123. Education N. Cell Adhesion and Cell Communication. 2010.
124. Bates ER and Nallamothu BK. Commentary: the role of percutaneous coronary intervention in ST-segment-elevation myocardial infarction. *Circulation.* 2008;118:567-73.
125. Rathore SS, Curtis JP, Chen J, Wang Y, Nallamothu BK, Epstein AJ and Krumholz HM. Association of door-to-balloon time and mortality in patients admitted to hospital with ST elevation myocardial infarction: national cohort study. *BMJ.* 2009;338:b1807.
126. Bradley EH, Nallamothu BK, Stern AF, Cherlin EJ, Wang Y, Byrd JR, Linnander EL, Nazem AG, Brush JE, Jr. and Krumholz HM. The door-to-balloon alliance for quality: who joins national collaborative efforts and why? *Joint Commission journal on quality and patient safety.* 2009;35:93-9.
127. Antman EM, Anbe DT, Armstrong PW, Bates ER, Green LA, Hand M, Hochman JS, Krumholz HM, Kushner FG, Lamas GA, Mullany CJ, Ornato JP, Pearle DL, Sloan MA, Smith SC, Jr., Alpert JS, Anderson JL, Faxon DP, Fuster V, Gibbons RJ, Gregoratos G, Halperin JL, Hiratzka LF, Hunt SA, Jacobs AK and Ornato JP. ACC/AHA guidelines for the management of patients with ST-elevation myocardial infarction; A report of the American College of Cardiology/American Heart Association Task Force on Practice Guidelines (Committee to Revise the 1999 Guidelines for the Management of patients with acute myocardial infarction). *Journal of the American College of Cardiology.* 2004;44:E1-e211.
128. Bonnefoy E, Steg PG, Boutitie F, Dubien PY, Lapostolle F, Roncalli J, Dissait F, Vanzetto G, Leizorowicz A, Kirkorian G, Mercier C, McFadden EP and Touboul P.

- Comparison of primary angioplasty and pre-hospital fibrinolysis in acute myocardial infarction (CAPTIM) trial: a 5-year follow-up. *European heart journal*. 2009;30:1598-606.
129. Björklund E, Stenstrand U, Lindbäck J, Svensson L, Wallentin L and Lindahl B. Pre-hospital thrombolysis delivered by paramedics is associated with reduced time delay and mortality in ambulance-transported real-life patients with ST-elevation myocardial infarction. *European heart journal*. 2006;27:1146-52.
130. Danchin N, Blanchard D, Steg PG, Sauval P, Hanania G, Goldstein P, Cambou JP, Guéret P, Vaur L, Boutalbi Y, Genès N and Lablanche JM. Impact of prehospital thrombolysis for acute myocardial infarction on 1-year outcome: results from the French Nationwide USIC 2000 Registry. *Circulation*. 2004;110:1909-15.
131. Serebruany VL, Steinhubl SR, Berger PB, Malinin AI, Baggish JS, Bhatt DL and Topol EJ. Analysis of risk of bleeding complications after different doses of aspirin in 192,036 patients enrolled in 31 randomized controlled trials. *The American journal of cardiology*. 2005;95:1218-22.
132. Chen ZM, Jiang LX, Chen YP, Xie JX, Pan HC, Peto R, Collins R and Liu LS. Addition of clopidogrel to aspirin in 45,852 patients with acute myocardial infarction: randomised placebo-controlled trial. *Lancet (London, England)*. 2005;366:1607-21.
133. Eisenberg PR. Role of heparin in coronary thrombolysis. *Chest*. 1992;101:131s-139s.
134. Keeley EC, Boura JA and Grines CL. Primary angioplasty versus intravenous thrombolytic therapy for acute myocardial infarction: a quantitative review of 23 randomised trials. *Lancet (London, England)*. 2003;361:13-20.
135. Pinto DS, Frederick PD, Chakrabarti AK, Kirtane AJ, Ullman E, Dejam A, Miller DP, Henry TD and Gibson CM. Benefit of transferring ST-segment-elevation myocardial infarction patients for percutaneous coronary intervention compared with administration of onsite fibrinolytic declines as delays increase. *Circulation*. 2011;124:2512-21.
136. Niccoli G, Burzotta F, Galiuto L and Crea F. Myocardial no-reflow in humans. *Journal of the American College of Cardiology*. 2009;54:281-92.
137. Nordmann AJ, Hengstler P, Harr T, Young J and Bucher HC. Clinical outcomes of primary stenting versus balloon angioplasty in patients with myocardial infarction: a meta-analysis of randomized controlled trials. *The American journal of medicine*. 2004;116:253-62.
138. Kastrati A, Dibra A, Spaulding C, Laarman GJ, Menichelli M, Valgimigli M, Di Lorenzo E, Kaiser C, Tierala I, Mehilli J, Seyfarth M, Varenne O, Dirksen MT, Percoco G, Varricchio A, Pittl U, Syvänne M, Suttrop MJ, Violini R and Schömig A. Meta-analysis of randomized trials on drug-eluting stents vs. bare-metal stents in patients with acute myocardial infarction. *European heart journal*. 2007;28:2706-13.
139. Sabate M, Cequier A, Iñiguez A, Serra A, Hernandez-Antolin R, Mainar V, Valgimigli M, Tsepili M, den Heijer P, Bethencourt A, Vazquez N, Gómez-Hospital JA, Baz JA, Martin-Yuste V, van Geuns RJ, Alfonso F, Bordes P, Tebaldi M, Masotti M, Silvestro A, Backx B, Brugaletta S, van Es GA and Serruys PW. Everolimus-eluting stent versus bare-metal stent in ST-segment elevation myocardial infarction (EXAMINATION): 1 year results of a randomised controlled trial. *Lancet (London, England)*. 2012;380:1482-90.
140. de Belder A, de la Torre Hernandez JM, Lopez-Palop R, O'Kane P, Hernandez Hernandez F, Strange J, Gimeno F, Cotton J, Diaz Fernandez JF, Carrillo Saez P, Thomas M, Pinar E, Curzen N, Baz JA, Cooter N, Lozano I, Skipper N, Robinson D and Hildick-Smith D. A prospective randomized trial of everolimus-eluting stents versus bare-metal stents in octogenarians: the XIMA Trial (Xience or Vision Stents for the Management of Angina in the Elderly). *Journal of the American College of Cardiology*. 2014;63:1371-5.

141. Seals DF and Courtneidge SA. The ADAMs family of metalloproteases: multidomain proteins with multiple functions. *Genes & development*. 2003;17:7-30.
142. Chute M, Jana S and Kassiri Z. Disintegrin and metalloproteinases (ADAMs and ADAM-TSs), the emerging family of proteases in heart physiology and pathology. *Current Opinion in Physiology*. 2018;1:34-45.
143. Endres K and Deller T. Regulation of Alpha-Secretase ADAM10 In vitro and In vivo: Genetic, Epigenetic, and Protein-Based Mechanisms. *Front Mol Neurosci*. 2017;10:56-56.
144. Gonzales PE, Solomon A, Miller AB, Leesnitzer MA, Sagi I and Milla ME. Inhibition of the tumor necrosis factor-alpha-converting enzyme by its pro domain. *The Journal of biological chemistry*. 2004;279:31638-45.
145. Leonard JD, Lin F and Milla ME. Chaperone-like properties of the prodomain of TNFalpha-converting enzyme (TACE) and the functional role of its cysteine switch. *The Biochemical journal*. 2005;387:797-805.
146. Moss ML, Bomar M, Liu Q, Sage H, Dempsey P, Lenhart PM, Gillispie PA, Stoeck A, Wildeboer D, Bartsch JW, Palmisano R and Zhou P. The ADAM10 prodomain is a specific inhibitor of ADAM10 proteolytic activity and inhibits cellular shedding events. *The Journal of biological chemistry*. 2007;282:35712-21.
147. Ngora H, Galli UM, Miyazaki K and Zöller M. Membrane-bound and exosomal metastasis-associated C4.4A promotes migration by associating with the $\alpha(6)\beta(4)$ integrin and MT1-MMP. *Neoplasia*. 2012;14:95-107.
148. Zhou A, Webb G, Zhu X and Steiner DF. Proteolytic processing in the secretory pathway. *The Journal of biological chemistry*. 1999;274:20745-8.
149. López-Otín C and Overall CM. Protease degradomics: a new challenge for proteomics. *Nat Rev Mol Cell Biol*. 2002;3:509-19.
150. Shi Z, Xu W, Loechel F, Wewer UM and Murphy LJ. ADAM 12, a disintegrin metalloprotease, interacts with insulin-like growth factor-binding protein-3. *The Journal of biological chemistry*. 2000;275:18574-80.
151. Roy R, Wewer UM, Zurakowski D, Pories SE and Moses MA. ADAM 12 cleaves extracellular matrix proteins and correlates with cancer status and stage. *The Journal of biological chemistry*. 2004;279:51323-30.
152. Huang J, Bridges LC and White JM. Selective modulation of integrin-mediated cell migration by distinct ADAM family members. *Molecular biology of the cell*. 2005;16:4982-4991.
153. Tomczuk M, Takahashi Y, Huang J, Murase S, Mistretta M, Klaffky E, Sutherland A, Bolling L, Coonrod S, Marcinkiewicz C, Sheppard D, Stepp MA and White JM. Role of multiple beta1 integrins in cell adhesion to the disintegrin domains of ADAMs 2 and 3. *Exp Cell Res*. 2003;290:68-81.
154. Bridges LC, Sheppard D and Bowditch RD. ADAM disintegrin-like domain recognition by the lymphocyte integrins alpha4beta1 and alpha4beta7. *The Biochemical journal*. 2005;387:101-8.
155. Ridley AJ, Schwartz MA, Burridge K, Firtel RA, Ginsberg MH, Borisy G, Parsons JT and Horwitz AR. Cell migration: integrating signals from front to back. *Science*. 2003;302:1704-9.
156. Lu D, Scully M, Kakkar V and Lu X. ADAM-15 disintegrin-like domain structure and function. *Toxins (Basel)*. 2010;2:2411-2427.
157. Thodeti CK, Albrechtsen R, Grauslund M, Asmar M, Larsson C, Takada Y, Mercurio AM, Couchman JR and Wewer UM. ADAM12/syndecan-4 signaling promotes beta 1 integrin-dependent cell spreading through protein kinase Calpha and RhoA. *The Journal of biological chemistry*. 2003;278:9576-84.

158. Gaultier A, Cousin H, Darribère T and Alfandari D. ADAM13 disintegrin and cysteine-rich domains bind to the second heparin-binding domain of fibronectin. *The Journal of biological chemistry*. 2002;277:23336-44.
159. Reddy P, Slack JL, Davis R, Cerretti DP, Kozlosky CJ, Blanton RA, Shows D, Peschon JJ and Black RA. Functional analysis of the domain structure of tumor necrosis factor-alpha converting enzyme. *The Journal of biological chemistry*. 2000;275:14608-14.
160. Takeda S, Igarashi T, Mori H and Araki S. Crystal structures of VAP1 reveal ADAMs' MDC domain architecture and its unique C-shaped scaffold. *EMBO J*. 2006;25:2388-2396.
161. Takeda S. Three-dimensional domain architecture of the ADAM family proteinases. *Seminars in cell & developmental biology*. 2009;20:146-52.
162. Zhong JL, Poghosyan Z, Pennington CJ, Scott X, Handsley MM, Warn A, Gavrilovic J, Honert K, Krüger A, Span PN, Sweep FC and Edwards DR. Distinct functions of natural ADAM-15 cytoplasmic domain variants in human mammary carcinoma. *Molecular cancer research : MCR*. 2008;6:383-94.
163. Sun C, Wu MH, Lee ES and Yuan SY. A disintegrin and metalloproteinase 15 contributes to atherosclerosis by mediating endothelial barrier dysfunction via Src family kinase activity. *Arteriosclerosis, thrombosis, and vascular biology*. 2012;32:2444-51.
164. Herren B, Raines EW and Ross R. Expression of a disintegrin-like protein in cultured human vascular cells and in vivo. *FASEB J*. 1997;11:173-80.
165. Horiuchi K, Weskamp G, Lum L, Hammes HP, Cai H, Brodie TA, Ludwig T, Chiusaroli R, Baron R, Preissner KT, Manova K and Blobel CP. Potential role for ADAM15 in pathological neovascularization in mice. *Mol Cell Biol*. 2003;23:5614-24.
166. Li JK, Du WJ, Jiang SL and Tian H. Expression of ADAM-15 in rat myocardial infarction. *Int J Exp Pathol*. 2009;90:347-354.
167. Arndt M, Lendeckel U, Röcken C, Nepple K, Wolke C, Spiess A, Huth C, Ansorge S, Klein HU and Goette A. Altered expression of ADAMs (A Disintegrin And Metalloproteinase) in fibrillating human atria. *Circulation*. 2002;105:720-5.
168. Sun C, Wu MH, Guo M, Day ML, Lee ES and Yuan SY. ADAM15 regulates endothelial permeability and neutrophil migration via Src/ERK1/2 signalling. *Cardiovasc Res*. 2010;87:348-55.
169. Xie B, Shen J, Dong A, Swaim M, Hackett SF, Wyder L, Worpenberg S, Barbieri S and Campochiaro PA. An Adam15 amplification loop promotes vascular endothelial growth factor-induced ocular neovascularization. *FASEB J*. 2008;22:2775-83.
170. Yang X, Meegan JE, Jannaway M, Coleman DC and Yuan SY. A disintegrin and metalloproteinase 15-mediated glycocalyx shedding contributes to vascular leakage during inflammation. *Cardiovascular research*. 2018;114:1752-1763.
171. Takawale A, Zhang P, Azad A, Wang W, Wang X, Murray AG and Kassiri Z. Myocardial overexpression of TIMP3 after myocardial infarction exerts beneficial effects by promoting angiogenesis and suppressing early proteolysis. *American journal of physiology Heart and circulatory physiology*. 2017;313:H224-h236.
172. Lang RM, Badano LP, Mor-Avi V, Afilalo J, Armstrong A, Ernande L, Flachskampf FA, Foster E, Goldstein SA, Kuznetsova T, Lancellotti P, Muraru D, Picard MH, Rietzschel ER, Rudski L, Spencer KT, Tsang W and Voigt JU. Recommendations for cardiac chamber quantification by echocardiography in adults: an update from the American Society of Echocardiography and the European Association of Cardiovascular Imaging. *Journal of the American Society of Echocardiography : official publication of the American Society of Echocardiography*. 2015;28:1-39.e14.
173. Iyer RP, de Castro Brás LE, Cannon PL, Ma Y, DeLeon-Pennell KY, Jung M, Flynn ER, Henry JB, Bratton DR, White JA, Fulton LK, Grady AW and Lindsey ML.

- Defining the sham environment for post-myocardial infarction studies in mice. *American journal of physiology Heart and circulatory physiology*. 2016;311:H822-36.
174. Thomas A, Gary AC, Christopher OM, Wade E, Xiaomeng T, James HA and Gail LM. Multiphoton and harmonic generation imaging methods enable direct visualization of drug nanoparticle carriers in conjunction with vasculature in fibrotic prostate tumor mouse model. *ProcSPIE*. 2019;10881.
175. Fan D, Takawale A, Basu R, Patel V, Lee J, Kandaram V, Wang X, Oudit GY and Kassiri Z. Differential role of TIMP2 and TIMP3 in cardiac hypertrophy, fibrosis, and diastolic dysfunction. *Cardiovasc Res*. 2014;103:268-80.
176. Epelman S, Liu PP and Mann DL. Role of innate and adaptive immune mechanisms in cardiac injury and repair. *Nature reviews Immunology*. 2015;15:117-29.
177. van Dijk A, Niessen HWM, Ursem W, Twisk JWR, Visser FC and van Milligen FJ. Accumulation of fibronectin in the heart after myocardial infarction: a putative stimulator of adhesion and proliferation of adipose-derived stem cells. *Cell Tissue Res*. 2008;332:289-298.
178. Jagadeeshan S, Krishnamoorthy YR, Singhal M, Subramanian A, Mavuluri J, Lakshmi A, Roshini A, Baskar G, Ravi M, Joseph LD, Sadasivan K, Krishnan A, Nair AS, Venkatraman G and Rayala SK. Transcriptional regulation of fibronectin by p21-activated kinase-1 modulates pancreatic tumorigenesis. *Oncogene*. 2015;34:455-64.
179. Kalogeris T, Baines CP, Krenz M and Korthuis RJ. Cell biology of ischemia/reperfusion injury. *Int Rev Cell Mol Biol*. 2012;298:229-317.
180. Valiente-Alandi I, Potter SJ, Salvador AM, Schafer AE, Schips T, Carrillo-Salinas F, Gibson AM, Nieman ML, Perkins C, Sargent MA, Huo J, Lorenz JN, DeFalco T, Molkentin JD, Alcaide P and Blaxall BC. Inhibiting Fibronectin Attenuates Fibrosis and Improves Cardiac Function in a Model of Heart Failure. *Circulation*. 2018;138:1236-1252.
181. Talman V and Ruskoaho H. Cardiac fibrosis in myocardial infarction-from repair and remodeling to regeneration. *Cell Tissue Res*. 2016;365:563-581.
182. Vainio LE, Szabó Z, Lin R, Ulvila J, Yrjölä R, Alakoski T, Piihola J, Koch WJ, Ruskoaho H, Fouse SD, Seeley TW, Gao E, Signore P, Lipson KE, Magga J and Kerkelä R. Connective Tissue Growth Factor Inhibition Enhances Cardiac Repair and Limits Fibrosis After Myocardial Infarction. *JACC: Basic to Translational Science*. 2019;4:83.
183. DeLeon-Pennell KY, Iyer RP, Ero OK, Cates CA, Flynn ER, Cannon PL, Jung M, Shannon D, Garrett MR, Buchanan W, Hall ME, Ma Y and Lindsey ML. Periodontal-induced chronic inflammation triggers macrophage secretion of Ccl12 to inhibit fibroblast-mediated cardiac wound healing. *JCI insight*. 2017;2.
184. Zidar N, Jeruc J, Balazic J and Stajer D. Neutrophils in human myocardial infarction with rupture of the free wall. *Cardiovascular pathology : the official journal of the Society for Cardiovascular Pathology*. 2005;14:247-50.
185. Shiraishi M, Shintani Y, Shintani Y, Ishida H, Saba R, Yamaguchi A, Adachi H, Yashiro K and Suzuki K. Alternatively activated macrophages determine repair of the infarcted adult murine heart. *J Clin Invest*. 2016;126:2151-66.
186. Abbate A, Salloum FN, Van Tassell BW, Vecile E, Toldo S, Seropian I, Mezzaroma E and Dobrina A. Alterations in the interleukin-1/interleukin-1 receptor antagonist balance modulate cardiac remodeling following myocardial infarction in the mouse. *PLoS One*. 2011;6:e27923.
187. Karpiński L, Płaksej R, Kosmala W and Witkowska M. Serum levels of interleukin-6, interleukin-10 and C-reactive protein in relation to left ventricular function in patients with myocardial infarction treated with primary angioplasty. *Kardiologia polska*. 2008;66:1279-85.

188. Hilfiker-Kleiner D, Shukla P, Klein G, Schaefer A, Stapel B, Hoch M, Müller W, Scherr M, Theilmeyer G, Ernst M, Hilfiker A and Drexler H. Continuous glycoprotein-130-mediated signal transducer and activator of transcription-3 activation promotes inflammation, left ventricular rupture, and adverse outcome in subacute myocardial infarction. *Circulation*. 2010;122:145-55.
189. Sun S, Sursal T, Adibnia Y, Zhao C, Zheng Y, Li H, Otterbein LE, Hauser CJ and Itagaki K. Mitochondrial DAMPs increase endothelial permeability through neutrophil dependent and independent pathways. *PloS one*. 2013;8:e59989-e59989.
190. Benson V, McMahon AC and Lowe HC. ICAM-1 in acute myocardial infarction: a potential therapeutic target. *Current molecular medicine*. 2007;7:219-27.
191. Clark PR, Manes TD, Pober JS and Kluger MS. Increased ICAM-1 expression causes endothelial cell leakiness, cytoskeletal reorganization and junctional alterations. *The Journal of investigative dermatology*. 2007;127:762-74.
192. Gao XM, White DA, Dart AM and Du XJ. Post-infarct cardiac rupture: recent insights on pathogenesis and therapeutic interventions. *Pharmacol Ther*. 2012;134:156-79.
193. Gao XM, Xu Q, Kiriazis H, Dart AM and Du XJ. Mouse model of post-infarct ventricular rupture: time course, strain- and gender-dependency, tensile strength, and histopathology. *Cardiovasc Res*. 2005;65:469-77.
194. Smith-Mungo LI and Kagan HM. Lysyl oxidase: properties, regulation and multiple functions in biology. *Matrix biology : journal of the International Society for Matrix Biology*. 1998;16:387-98.
195. Mao Y and Schwarzbauer JE. Fibronectin fibrillogenesis, a cell-mediated matrix assembly process. *Matrix biology : journal of the International Society for Matrix Biology*. 2005;24:389-99.
196. Knowlton AA, Connelly CM, Romo GM, Mamuya W, Apstein CS and Brecher P. Rapid expression of fibronectin in the rabbit heart after myocardial infarction with and without reperfusion. *J Clin Invest*. 1992;89:1060-8.
197. Casscells W, Kimura H, Sanchez JA, Yu ZX and Ferrans VJ. Immunohistochemical study of fibronectin in experimental myocardial infarction. *Am J Pathol*. 1990;137:801-10.
198. Lu W and Mayer BJ. Mechanism of activation of Pak1 kinase by membrane localization. *Oncogene*. 1999;18:797-806.
199. Kärkkäinen S, Hiipakka M, Wang J-H, Kleino I, Vähä-Jaakkola M, Renkema GH, Liss M, Wagner R and Saksela K. Identification of preferred protein interactions by phage-display of the human Src homology-3 proteome. *EMBO Rep*. 2006;7:186-191.
200. Poghosyan Z, Robbins SM, Houslay MD, Webster A, Murphy G and Edwards DR. Phosphorylation-dependent interactions between ADAM15 cytoplasmic domain and Src family protein-tyrosine kinases. *The Journal of biological chemistry*. 2002;277:4999-5007.
201. Yablonski D, Kane LP, Qian D and Weiss A. A Nck-Pak1 signaling module is required for T-cell receptor-mediated activation of NFAT, but not of JNK. *EMBO J*. 1998;17:5647-5657.
202. Ma QL, Yang F, Frautschy SA and Cole GM. PAK in Alzheimer disease, Huntington disease and X-linked mental retardation. *Cellular logistics*. 2012;2:117-125.
203. Roig J, Tuazon PT, Zipfel PA, Pendergast AM and Traugh JA. Functional interaction between c-Abl and the p21-activated protein kinase gamma-PAK. *Proceedings of the National Academy of Sciences of the United States of America*. 2000;97:14346-51.
204. Wynn TA. Cellular and molecular mechanisms of fibrosis. *J Pathol*. 2008;214:199-210.

205. Martin K, Pritchett J, Llewellyn J, Mullan AF, Athwal VS, Dobie R, Harvey E, Zeef L, Farrow S, Streuli C, Henderson NC, Friedman SL, Hanley NA and Piper Hanley K. PAK proteins and YAP-1 signalling downstream of integrin beta-1 in myofibroblasts promote liver fibrosis. *Nat Commun.* 2016;7:12502.
206. Bowers SLK, Davis-Rodriguez S, Thomas ZM, Rudomanova V, Bacon WC, Beiersdorfer A, Ma Q, Devarajan P and Blaxall BC. Inhibition of fibronectin polymerization alleviates kidney injury due to ischemia-reperfusion. *Am J Physiol Renal Physiol.* 2019;316:F1293-f1298.
207. Altrock E, Sens C, Wuerfel C, Vasel M, Kawelke N, Dooley S, Sottile J and Nakchbandi IA. Inhibition of fibronectin deposition improves experimental liver fibrosis. *J Hepatol.* 2015;62:625-33.
208. Medi C, Montalescot G, Budaj A, Fox KA, López-Sendón J, FitzGerald G and Brieger DB. Reperfusion in patients with renal dysfunction after presentation with ST-segment elevation or left bundle branch block: GRACE (Global Registry of Acute Coronary Events). *JACC Cardiovascular interventions.* 2009;2:26-33.
209. Ryou MG and Mallet RT. An In Vitro Oxygen-Glucose Deprivation Model for Studying Ischemia-Reperfusion Injury of Neuronal Cells. *Methods Mol Biol.* 2018;1717:229-235.
210. Vivar R, Humeres C, Ayala P, Olmedo I, Catalán M, García L, Lavandero S and Díaz-Araya G. TGF- β 1 prevents simulated ischemia/reperfusion-induced cardiac fibroblast apoptosis by activation of both canonical and non-canonical signaling pathways. *Biochimica et Biophysica Acta (BBA) - Molecular Basis of Disease.* 2013;1832:754-762.
211. Takawale A, Fan D, Basu R, Shen M, Parajuli N, Wang W, Wang X, Oudit GY and Kassiri Z. Myocardial recovery from ischemia-reperfusion is compromised in the absence of tissue inhibitor of metalloproteinase 4. *Circ Heart Fail.* 2014;7:652-62.
212. MacKenna D, Summerour SR and Villarreal FJ. Role of mechanical factors in modulating cardiac fibroblast function and extracellular matrix synthesis. *Cardiovasc Res.* 2000;46:257-63.
213. Carver W, Terracio L and Borg TK. Expression and accumulation of interstitial collagen in the neonatal rat heart. *Anat Rec.* 1993;236:511-20.
214. Villarreal FJ and Kim NN. Regulation of myocardial extracellular matrix components by mechanical and chemical growth factors. *Cardiovasc Pathol.* 1998;7:145-51.
215. Villarreal FJ and Dillmann WH. Cardiac hypertrophy-induced changes in mRNA levels for TGF-beta 1, fibronectin, and collagen. *Am J Physiol.* 1992;262:H1861-6.
216. Kuwahara F, Kai H, Tokuda K, Kai M, Takeshita A, Egashira K and Imaizumi T. Transforming growth factor-beta function blocking prevents myocardial fibrosis and diastolic dysfunction in pressure-overloaded rats. *Circulation.* 2002;106:130-5.
217. Petz A, Grandoch M, Gorski DJ, Abrams M, Piroth M, Schneckmann R, Homann S, Müller J, Hartwig S, Lehr S, Yamaguchi Y, Wight TN, Gorressen S, Ding Z, Kötter S, Krüger M, Heinen A, Kelm M, Gödecke A, Flögel U and Fischer JW. Cardiac Hyaluronan Synthesis Is Critically Involved in the Cardiac Macrophage Response and Promotes Healing After Ischemia Reperfusion Injury. *Circulation Research.* 2019;124:1433-1447.
218. Stern R, Shuster S, Neudecker BA and Formby B. Lactate stimulates fibroblast expression of hyaluronan and CD44: the Warburg effect revisited. *Exp Cell Res.* 2002;276:24-31.
219. Howard CM and Baudino TA. Dynamic cell-cell and cell-ECM interactions in the heart. *J Mol Cell Cardiol.* 2014;70:19-26.
220. Goldsmith EC, Bradshaw AD, Zile MR and Spinale FG. Myocardial fibroblast-matrix interactions and potential therapeutic targets. *J Mol Cell Cardiol.* 2014;70:92-9.

221. Eghbali M and Weber KT. Collagen and the myocardium: fibrillar structure, biosynthesis and degradation in relation to hypertrophy and its regression. *Mol Cell Biochem.* 1990;96:1-14.
222. Bashey RI, Donnelly M, Insinga F and Jimenez SA. Growth properties and biochemical characterization of collagens synthesized by adult rat heart fibroblasts in culture. *J Mol Cell Cardiol.* 1992;24:691-700.
223. Rohr S. Arrhythmogenic implications of fibroblast-myocyte interactions. *Circ Arrhythm Electrophysiol.* 2012;5:442-52.
224. Lee HW and Eghbali-Webb M. Estrogen enhances proliferative capacity of cardiac fibroblasts by estrogen receptor- and mitogen-activated protein kinase-dependent pathways. *J Mol Cell Cardiol.* 1998;30:1359-68.
225. Wang H, Zhao Z, Lin M and Groban L. Activation of GPR30 inhibits cardiac fibroblast proliferation. *Mol Cell Biochem.* 2015;405:135-48.
226. Pedram A, Razandi M, Narayanan R and Levin ER. Estrogen receptor beta signals to inhibition of cardiac fibrosis. *Mol Cell Endocrinol.* 2016;434:57-68.
227. Iorga A, Li J, Sharma S, Umar S, Bopassa JC, Nadadur RD, Centala A, Ren S, Saito T, Toro L, Wang Y, Stefani E and Eghbali M. Rescue of Pressure Overload-Induced Heart Failure by Estrogen Therapy. *J Am Heart Assoc.* 2016;5.